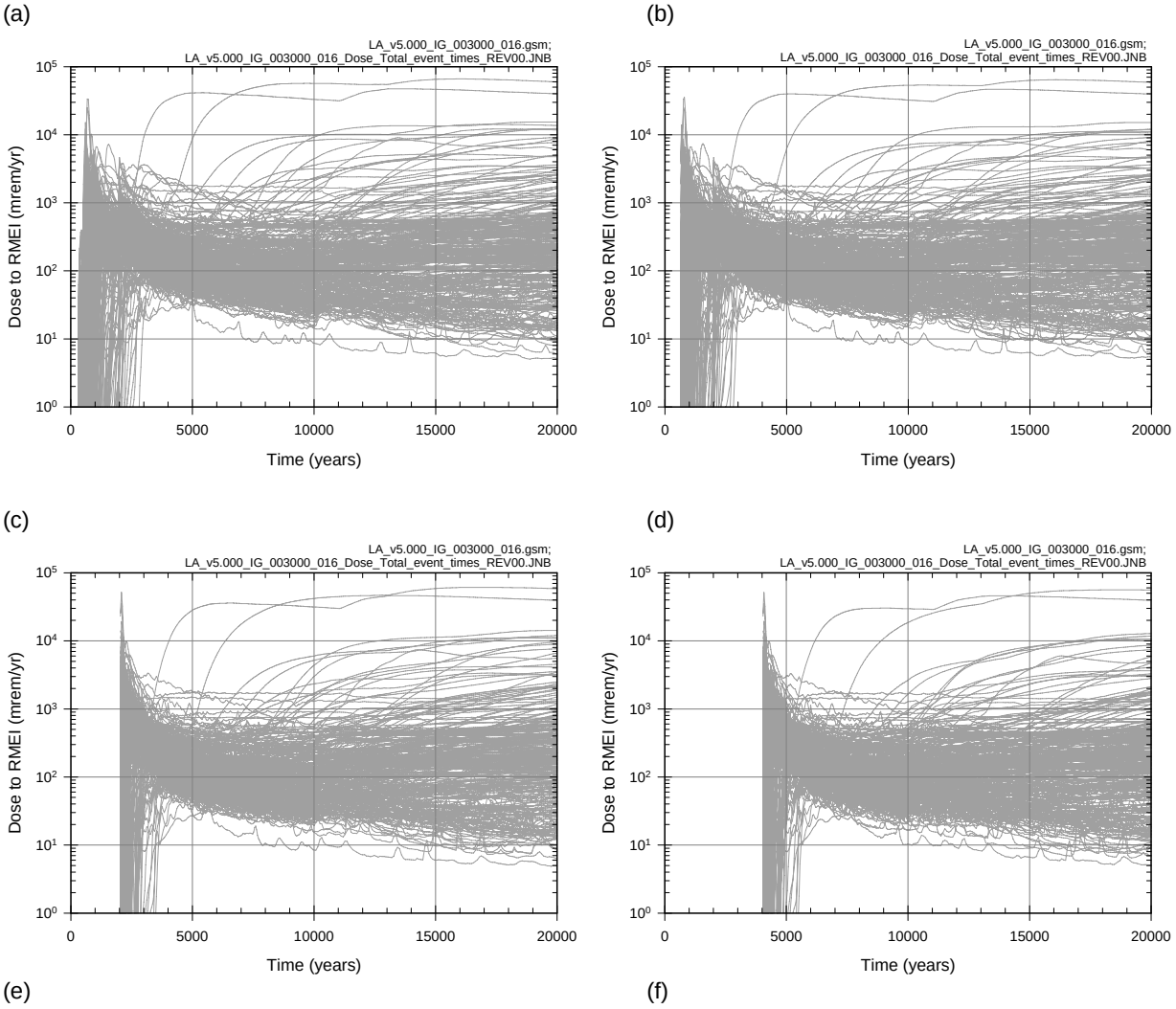

Source: Ouput DTNs: MO0709TSPAPLOT.000 [DIRS 183010]; and MO0709TSPAREGS.000 [DIRS 182976].

Figure J7.2-1. Dose to RMEI $D_{Il}(\tau|[1, t_k, nWP], \mathbf{e}_{Mi})$ from igneous intrusive events at times t_k = 10, 600, 2000, 4000, 6000 and 10,000 yr for i = 1, 2, …, $nLHS$ = 300: (a) 10 yr, (b) 600 yr, (c) 2000 yr, (d) 4000 yr, (e) 6000 yr, and (f) 10,000 yr.

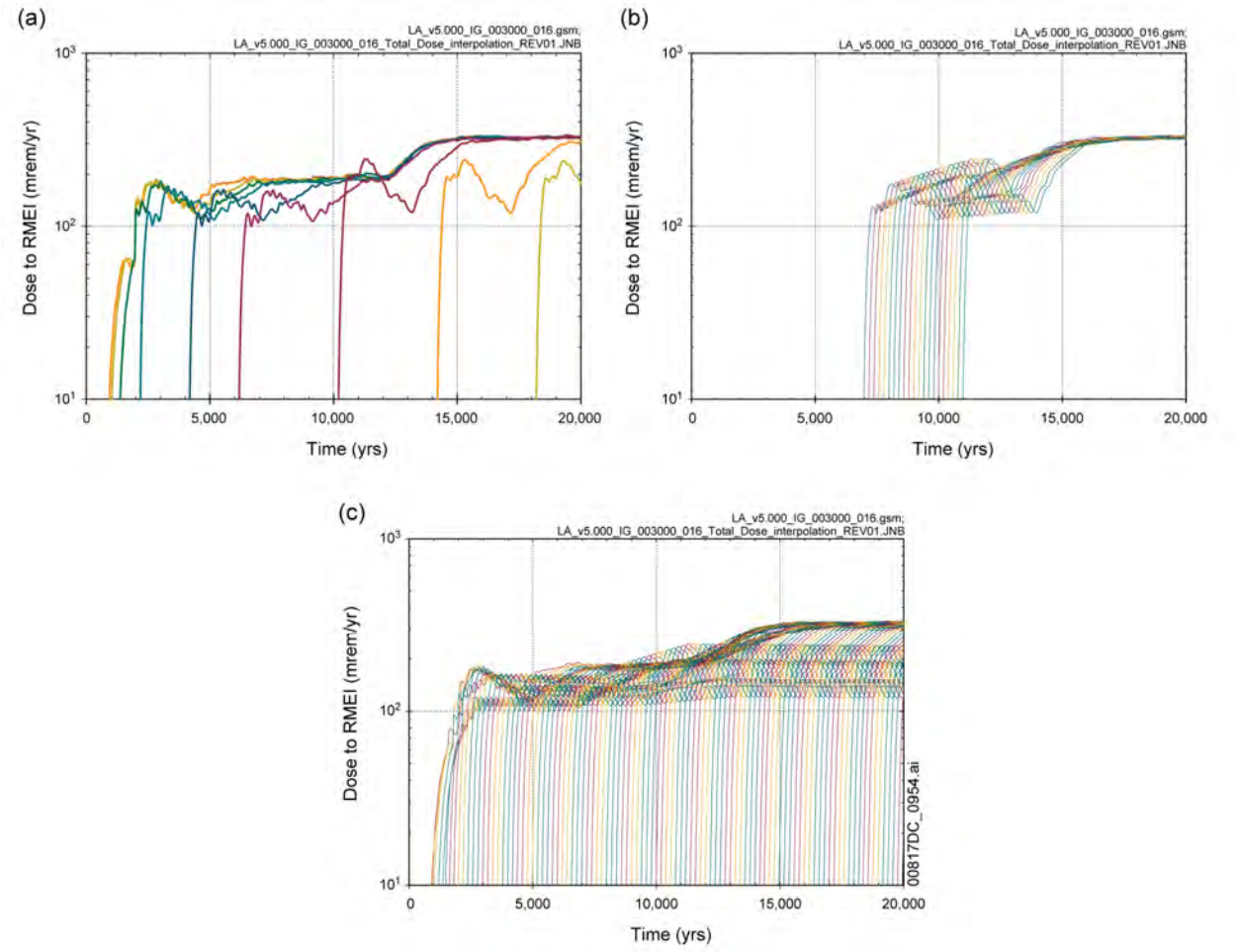

Source: Ouput DTNs: MO0709TSPAPLOT.000 [DIRS 183010]; and MO0709TSPAREGS.000 [DIRS 182976].

Figure J7.2-2. Illustration of interpolation procedure used to obtain estimated doses $\hat{D}_{II}(\tau|[1, \hat{t}_k, nWP], \mathbf{e}_{M1})$ from calculated doses $D_{II}(\tau|[1, t_k, nWP], \mathbf{e}_{M1})$ indicated in Equation J7.2-18 for LHS element $\mathbf{e}_1 = [\mathbf{e}_{A1}, \mathbf{e}_{M1}]$ and the time interval $[0, 2.0 \times 10^4$ yr]: (a) $D_{II}(\tau|[1, t_k, nWP], \mathbf{e}_{M1})$, $k = 1, 2, \ldots, 10$, (b) interpolated values $\hat{D}_{II}(\tau|[1, \hat{t}_k, nWP], \mathbf{e}_{M1})$ for $\hat{t}_k$ between $t_7 = 6000$ and $t_{8+1} = 10{,}000$, and (c) interpolated values $\hat{D}_{II}(\tau|[1, \hat{t}_k, nWP], \mathbf{e}_{M1})$ for $\hat{t}_k$ between 10 yr and 2.0×10^4 yr.

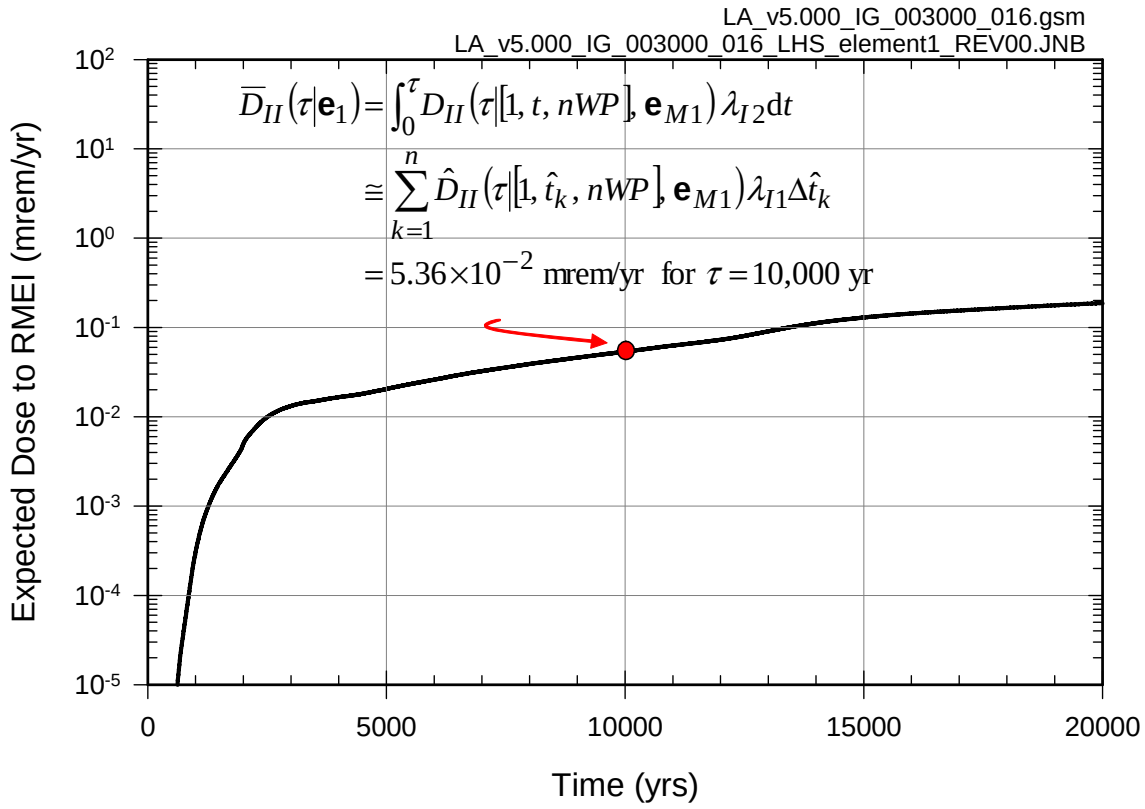

Source: Ouput DTNs: MO0709TSPAPLOT.000 [DIRS 183010]; and MO0709TSPAREGS.000 [DIRS 182976].

Figure J7.2-3. Determination of $\overline{D}_{II}(\tau|\mathbf{e}_1)$ as indicated in conjunction with Equations J7.2-7, J7.2-9 and J7.2-19 from calculated doses $D_{II}(\tau|[1, t_k, nWP], \mathbf{e}_{M1})$ shown in Equation J7.2-18 for LHS element $\mathbf{e}_1 = [\mathbf{e}_{A1}, \mathbf{e}_{M1}]$ and the time interval $[0, 2.0 \times 10^4$ yr].

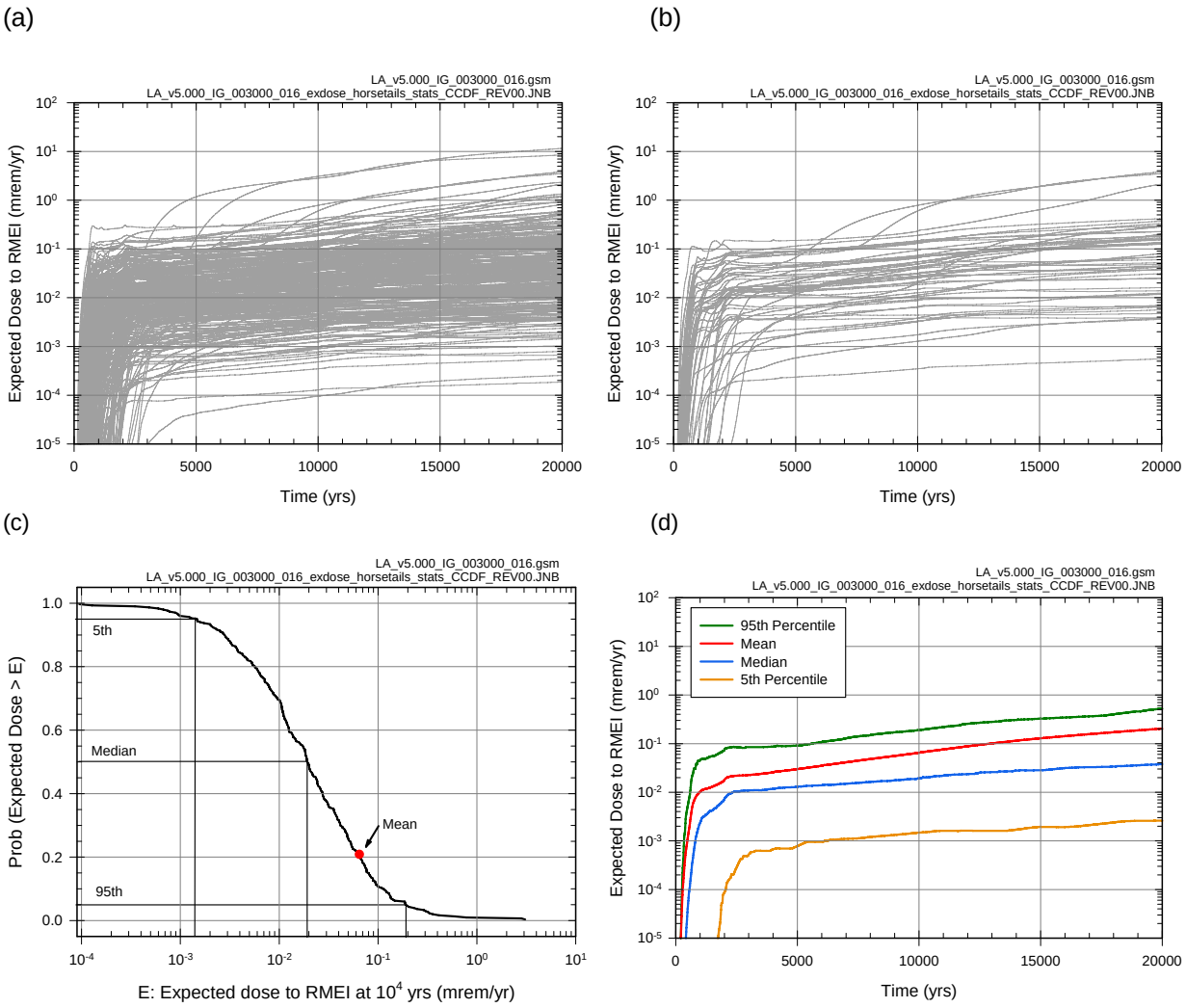

Source: Ouput DTNs: MO0709TSPAPLOT.000 [DIRS 183010]; and MO0709TSPAREGS.000 [DIRS 182976].

Figure J7.2-4. Estimate obtained with LHS of size *nLHS* = 300 showing epistemic uncertainty in expected dose $\bar{D}_{II}(\tau|\mathbf{e})$ to RMEI for $0 \le \tau \le 20{,}000$ yr that results when only igneous intrusion events are considered: (a) expected dose $\bar{D}_{II}(\tau|\mathbf{e}_i)$, i = 1, 2, …, *nLHS* = 300, (b) expected dose $\bar{D}_{II}(\tau|\mathbf{e}_i)$, i = 1, 2, …, 50, (c) exceedance probabilities $p_E[D < \bar{D}_{II}(\tau|\mathbf{e})]$ and quantiles $Q_q[\bar{D}_{II}(\tau|\mathbf{e})]$, q = 0.05, 0.5 and 0.95, for $\tau = 10^4$ yr, and (d) expected (mean) dose $\bar{D}_{II}(\tau)$ and quantiles $Q_q[\bar{D}_{II}(\tau|\mathbf{e})]$, q = 0.05, 0.5, 0.95.

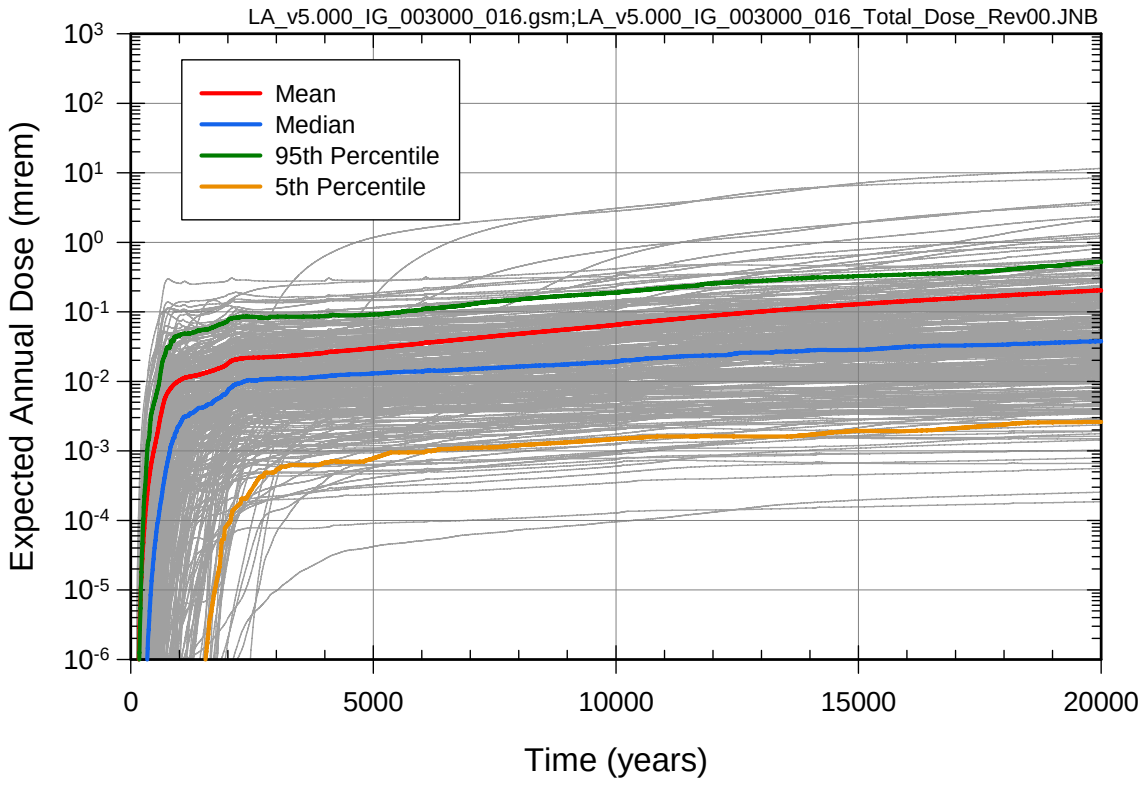

Source: Ouput DTNs: MO0709TSPAPLOT.000 [DIRS 183010]; and MO0709TSPAREGS.000 [DIRS 182976].

Figure J7.2-5. Summary presentation of epistemic uncertainty in expected dose $\bar{D}_{II}(\tau|\mathbf{e})$ to RMEI that results when only igneous intrusion is considered for $0 \leq \tau \leq 2.0 \times 10^4$ yr.

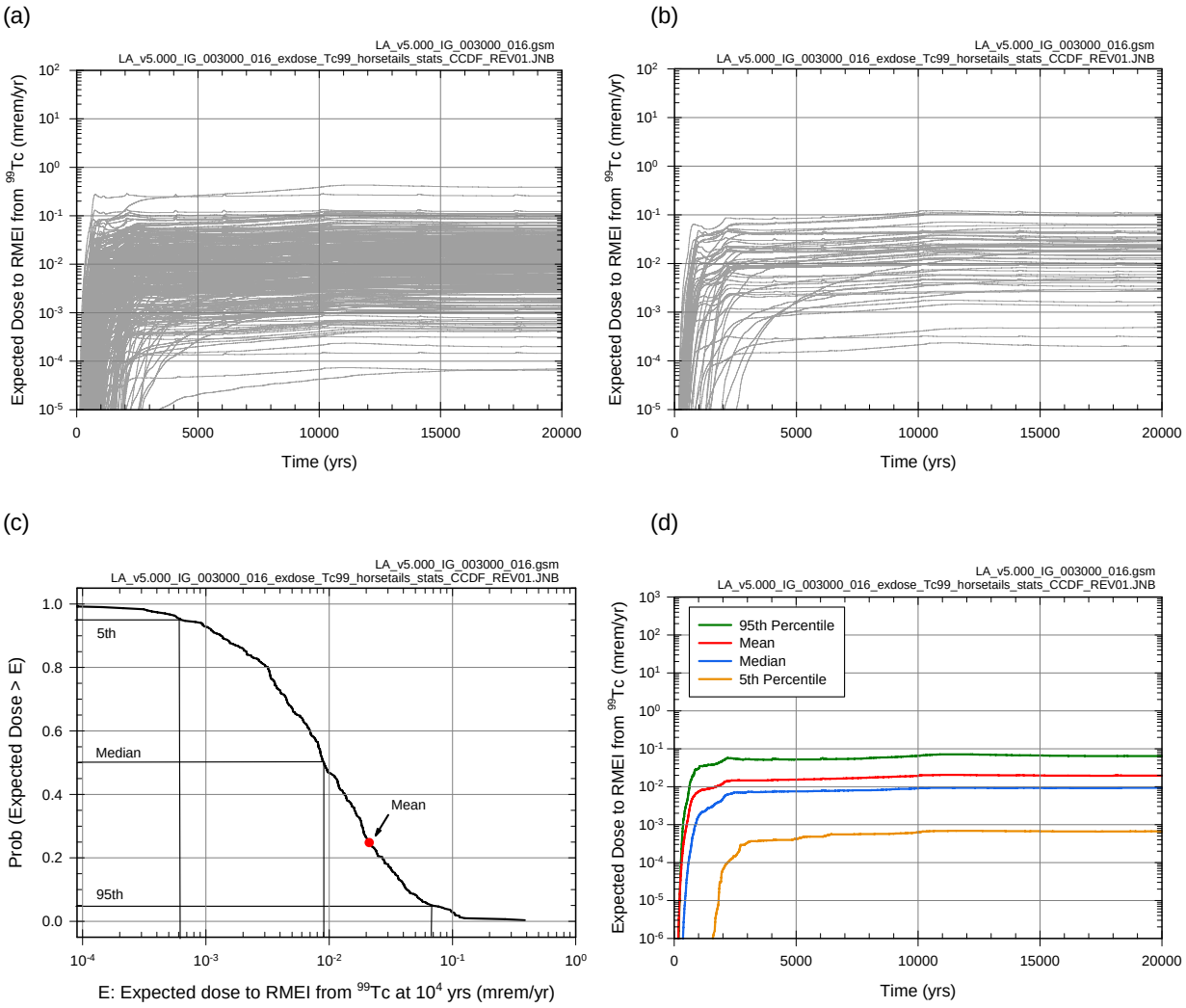

Source: Ouput DTNs: MO0709TSPAPLOT.000 [DIRS 183010]; and MO0709TSPAREGS.000 [DIRS 182976].

Figure J7.2-6. Estimate obtained with LHS of size *nLHS* = 300 showing epistemic uncertainty in expected dose $\bar{D}_{II,r}(\tau|\mathbf{e})$ to RMEI for $0 \le \tau \le 20{,}000$ yr with r corresponding to ^{99}Tc that results when only igneous intrusive events are considered: (a) expected dose $\bar{D}_{II,r}(\tau|\mathbf{e}_i)$, $i = 1, 2, \ldots, nLHS = 300$, (b) expected dose $\bar{D}_{II,r}(\tau|\mathbf{e}_i)$, $i = 1, 2, \ldots, 50$, (c) exceedance probabilities $p_E[D < \bar{D}_{II,r}(\tau|\mathbf{e})]$ and quantiles $Q_q[\bar{D}_{II,r}(\tau|\mathbf{e})]$, $q = 0.05$, 0.5 and 0.95, for $\tau = 10^4$ yr, and (d) expected (mean) dose $\bar{\bar{D}}_{II,r}(\tau)$ and quantiles $Q_q[\bar{D}_{II,r}(\tau|\mathbf{e})]$, $q = 0.05, 0.5, 0.95$.

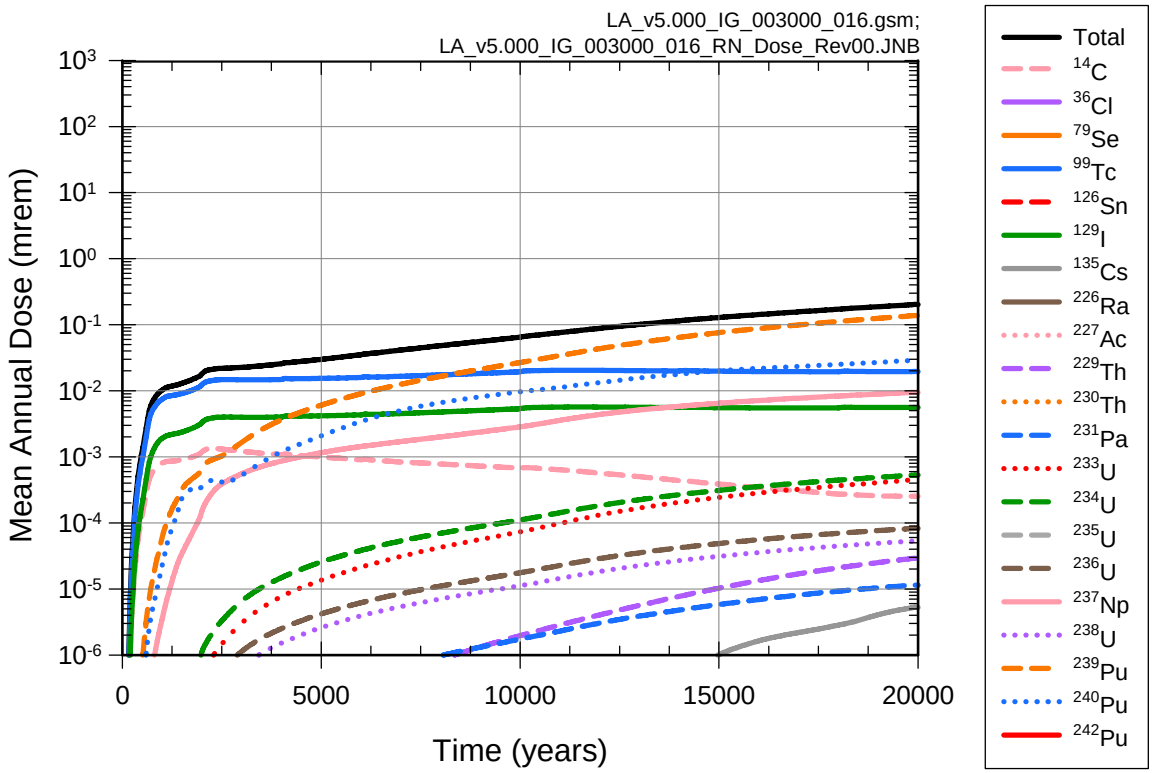

Source: Ouput DTNs: MO0709TSPAPLOT.000 [DIRS 183010]; and MO0709TSPAREGS.000 [DIRS 182976].

Figure J7.2-7. Estimates obtained with LHS of size *nLHS* = 300 of expected (mean) dose $\bar{\bar{D}}_{II,r}(\tau)$ to RMEI for $0 \leq \tau \leq 20{,}000$ yr for individual radioactive species that result when only igneous intrusive events are considered.

(a)

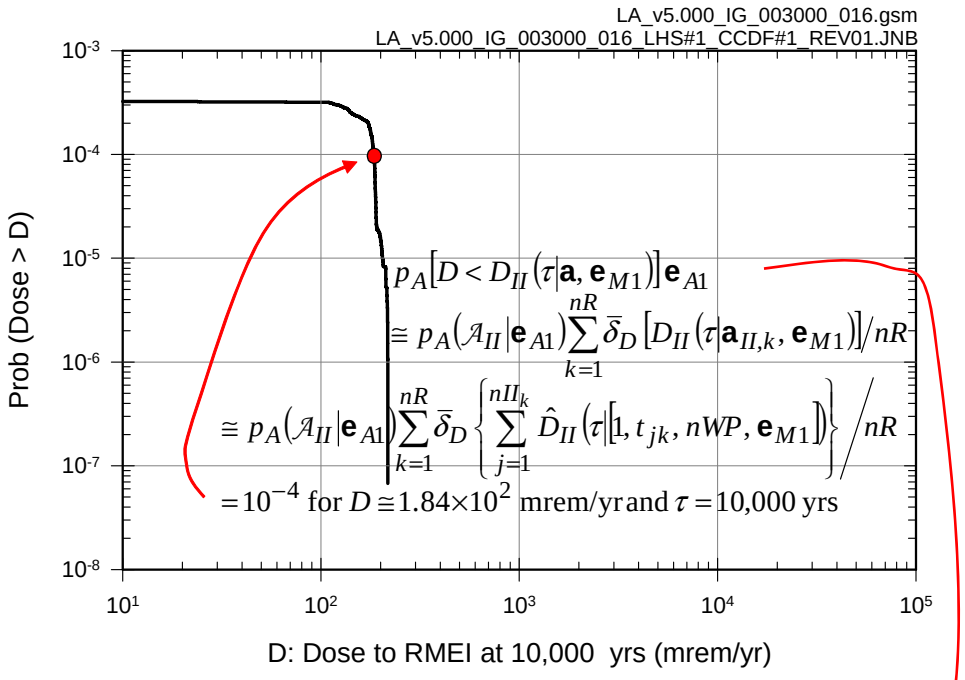

(b)

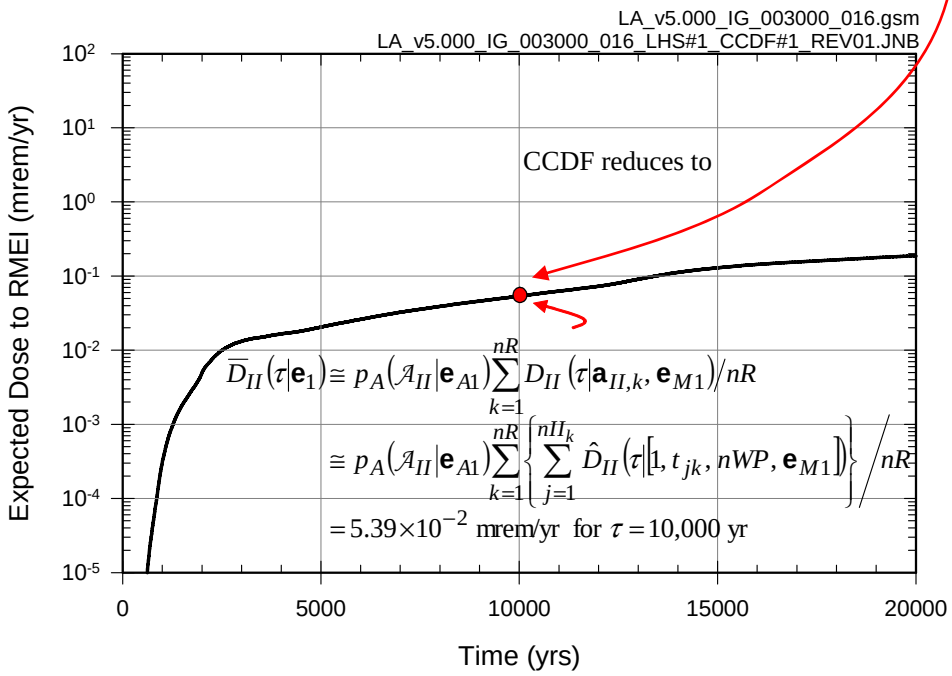

Source: Ouput DTNs: MO0709TSPAPLOT.000 [DIRS 183010]; and MO0709TSPAREGS.000 [DIRS 182976].

Figure J7.2-8. Results associated with $\bar{D}_{II}(\tau|\mathbf{e}_1)$ for LHS element $\mathbf{e}_1 = [\mathbf{e}_{A1}, \mathbf{e}_{M1}]$ obtained with sampling-based (Monte Carlo) procedures: (a) CCDF for $D_{II}(10^4 \text{ yr}|\mathbf{a}_{II}, \mathbf{e}_{M1})$ with exceedance probabilities $p_A[D < D_{II}(10^4 \text{ yr}|\mathbf{a}, \mathbf{e}_{M1})|\mathbf{e}_{A1}]$ defined in Equation J7.2-23, and (b) expected dose $\bar{D}_{II}(10^4 \text{ yr}|\mathbf{e}_1)$ associated with $D_{II}(10^4 \text{ yr}|\mathbf{a}_{II}, \mathbf{e}_{M1})$ as defined in Equation J7.2-21.

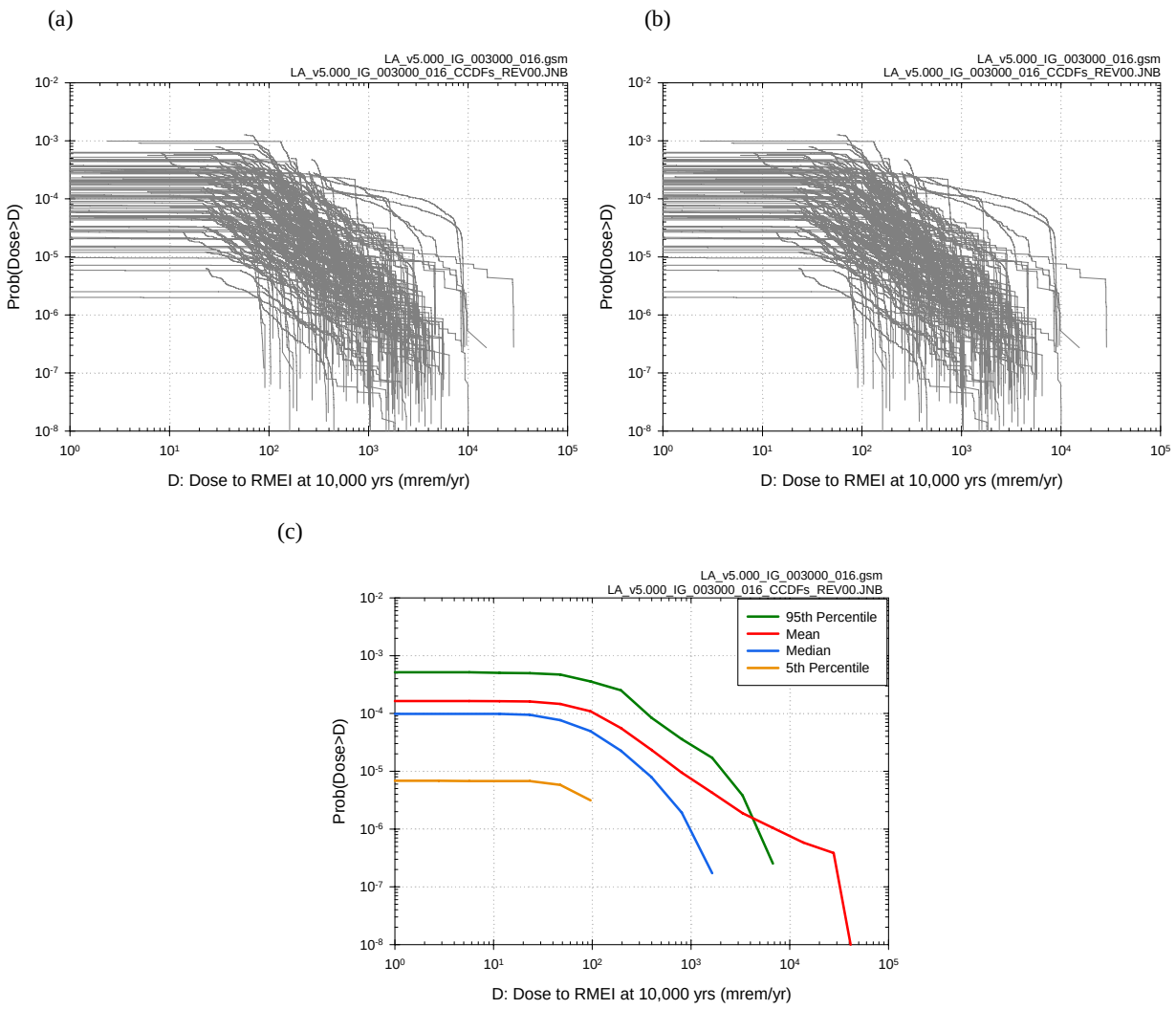

Source: Ouput DTNs: MO0709TSPAPLOT.000 [DIRS 183010]; and MO0709TSPAREGS.000 [DIRS 182976].

Figure J7.2-9. Results associated with $D_{II}(10^4 \text{ yr}|\mathbf{a}_{II}, \mathbf{e}_M)$ obtained with sampling-based (Monte Carlo) procedures for an LHS of size $nLHS = 300$: (a) CCDFs for $D_{II}(10^4 \text{ yr}|\mathbf{a}_{II}, \mathbf{e}_{Mi})$ with exceedance probabilities $p_A[D < D_{II}(10^4 \text{ yr}|\mathbf{a}, \mathbf{e}_{Mi})|\mathbf{e}_{Ai}]$ defined in Equation J7.2-23 for $i = 1, 2, \ldots, nLHS = 300$, (b) CCDFs for $D_{II}(10^4 \text{ yr}|\mathbf{a}_{II}, \mathbf{e}_{Mi})$ with exceedance probabilities $p_A[D < D_{II}(10^4 \text{ yr}|\mathbf{a}, \mathbf{e}_{Mi})|\mathbf{a}_{Ai}]$ defined in Equation J7.2-23 for $i = 1, 2, \ldots, 50$, and (c) expected (mean) CCDF and quantile curves, $q = 0.05, 0.5, 0.95$, for CCDFs in (a).

(a)

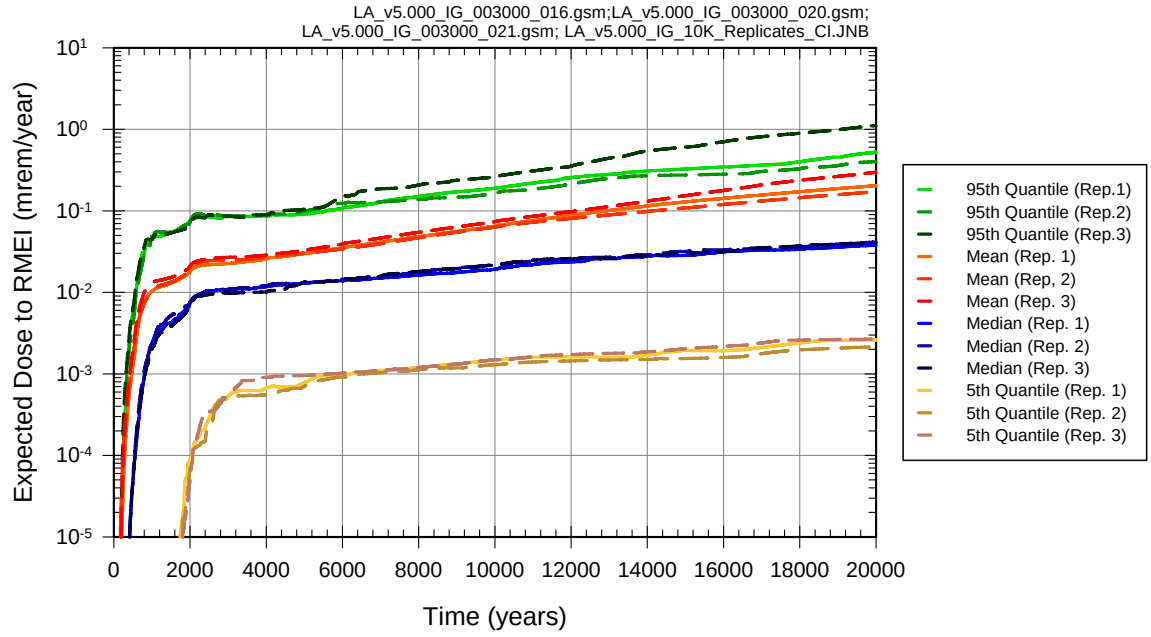

(b)

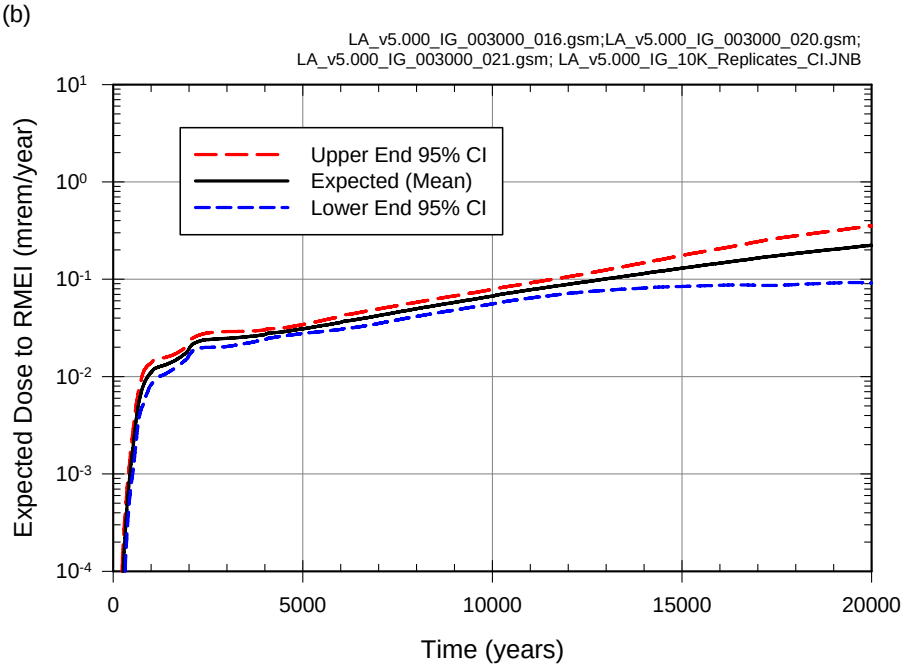

Source: Ouput DTNs: MO0709TSPAPLOT.000 [DIRS 183010]; MO0709TSPAREGS.000 [DIRS 182976]; and MO0709TSPASTAB.000 [DIRS 182983].

Figure J7.2-10. Assessment with replicated sampling of numerical error associated with use of an LHS of size *nLHS* = 300 to determine epistemic uncertainty in expected dose $\bar{D}_{II}(\tau|\mathbf{e})$ to RMEI for $0 \le \tau \le 20{,}000$ yr that results when only igneous intrusive events are considered: (a) Replicated estimates of expected (mean) dose $\bar{\bar{D}}_{II}(\tau)$ and quantiles $Q_q[\bar{D}_{II}(\tau|\mathbf{e})]$, q = 0.05, 0.5, 0.95, and (b) confidence intervals for estimates of expected (mean) dose $\bar{\bar{D}}_{II}(\tau)$.

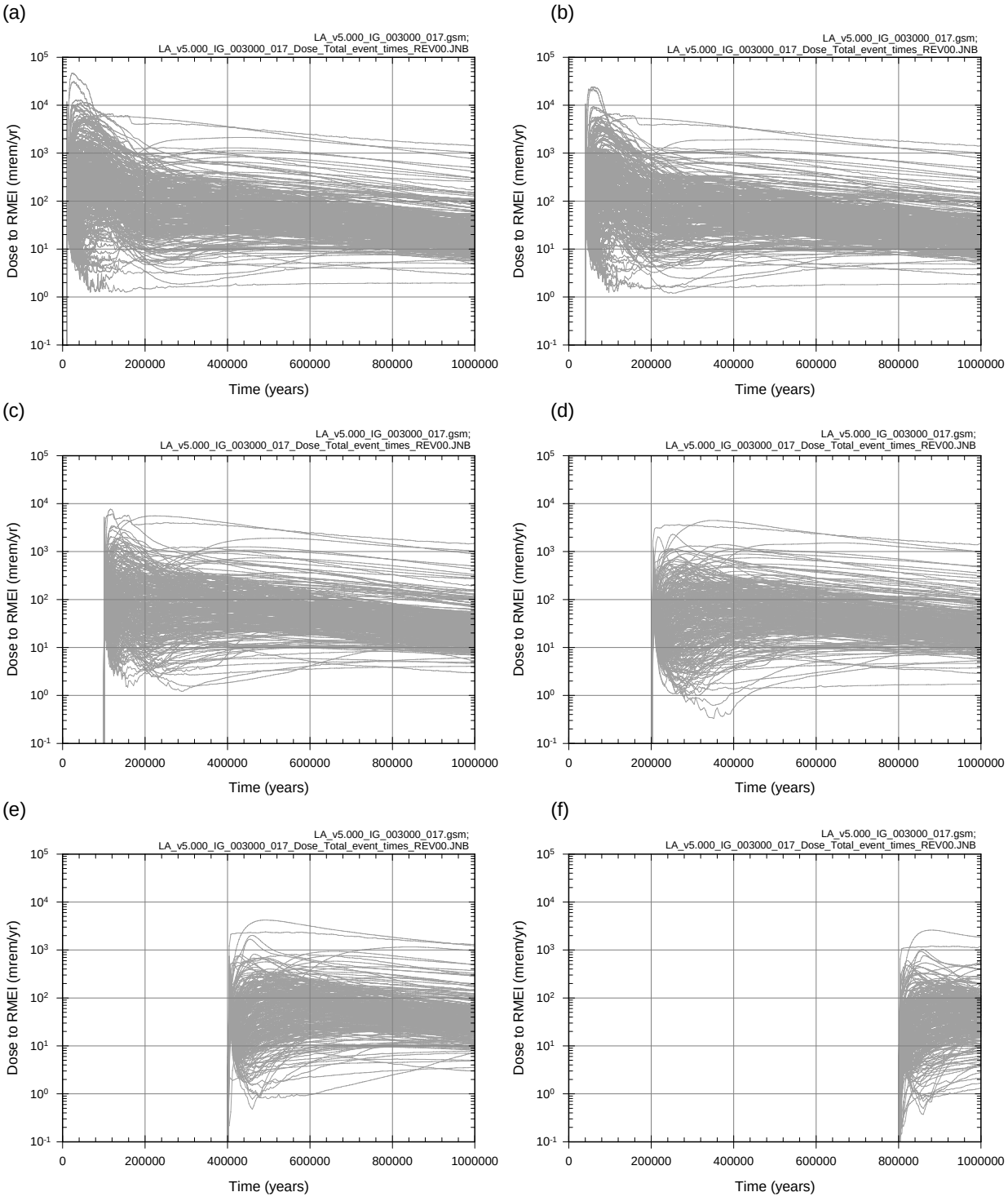

Source: Ouput DTNs: MO0709TSPAPLOT.000 [DIRS 183010]; and MO0709TSPAREGS.000 [DIRS 182976].

Figure J7.2-11. Dose to RMEI $D_{II}(\tau|[1, t_k, nWP], \mathbf{e}_{Mi})$ from igneous intrusive events at times t_k = 10,000, 40,000, 100,000, 200,000, 400,000 and 800,000 yr for i = 1, 2, …, $nLHS$ = 300: (a) 10,000 yr, (b) 40,000 yr, (c) 100,000 yr, (d) 200,000 yr, (e) 400,000 yr, and (f) 800,000 yr.

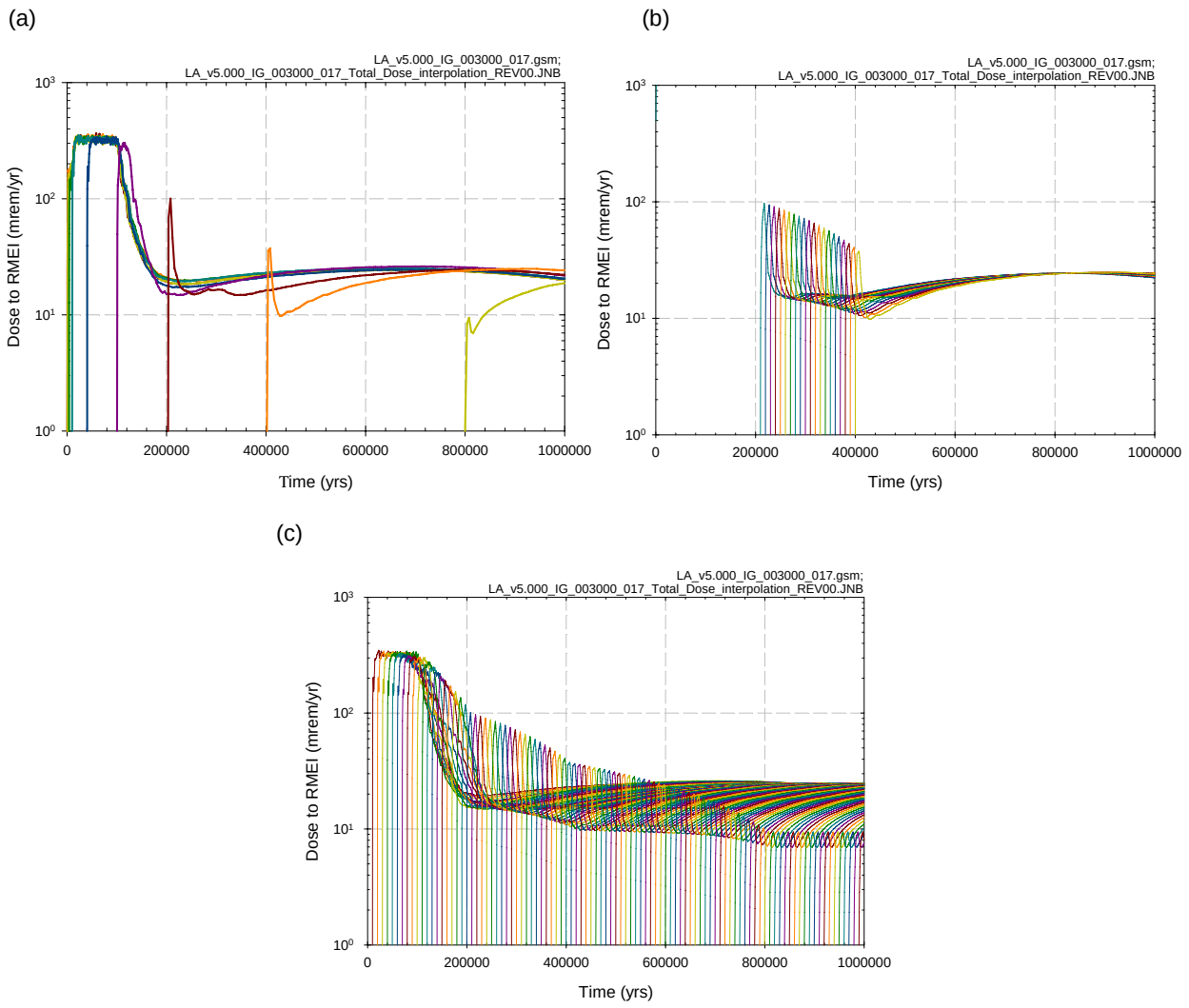

Source: Ouput DTNs: MO0709TSPAPLOT.000 [DIRS 183010]; and MO0709TSPAREGS.000 [DIRS 182976].

Figure J7.2-12. Illustration of interpolation procedure used to obtain estimated doses $\hat{D}_{II}(\tau|[1, \hat{t}_k, nWP], \mathbf{e}_{M1})$ from calculated doses $D_{II}(\tau|[1, t_k, nWP], \mathbf{e}_{M1})$ indicated in Equation J7.2-18 for LHS element $\mathbf{e}_1 = [\mathbf{e}_{A1}, \mathbf{e}_{M1}]$ and the time interval [0, 10^6 yr]: (a) $D_{II}(\tau|[1, t_k, nWP], \mathbf{e}_{M1})$, k = 1, 2, …, 10, (b) interpolated values $\hat{D}_{II}(\tau|[1, \hat{t}_k, nWP], \mathbf{e}_{M1})$ for $\hat{t}_k$ between t_8 = 200,000 yr and t_9= 400,000, and (c) interpolated values $\hat{D}_{II}(\tau|[1, \hat{t}_k, nWP], \mathbf{e}_{M1})$ for $\hat{t}_k$ between 250 yr and 10^6 yr.

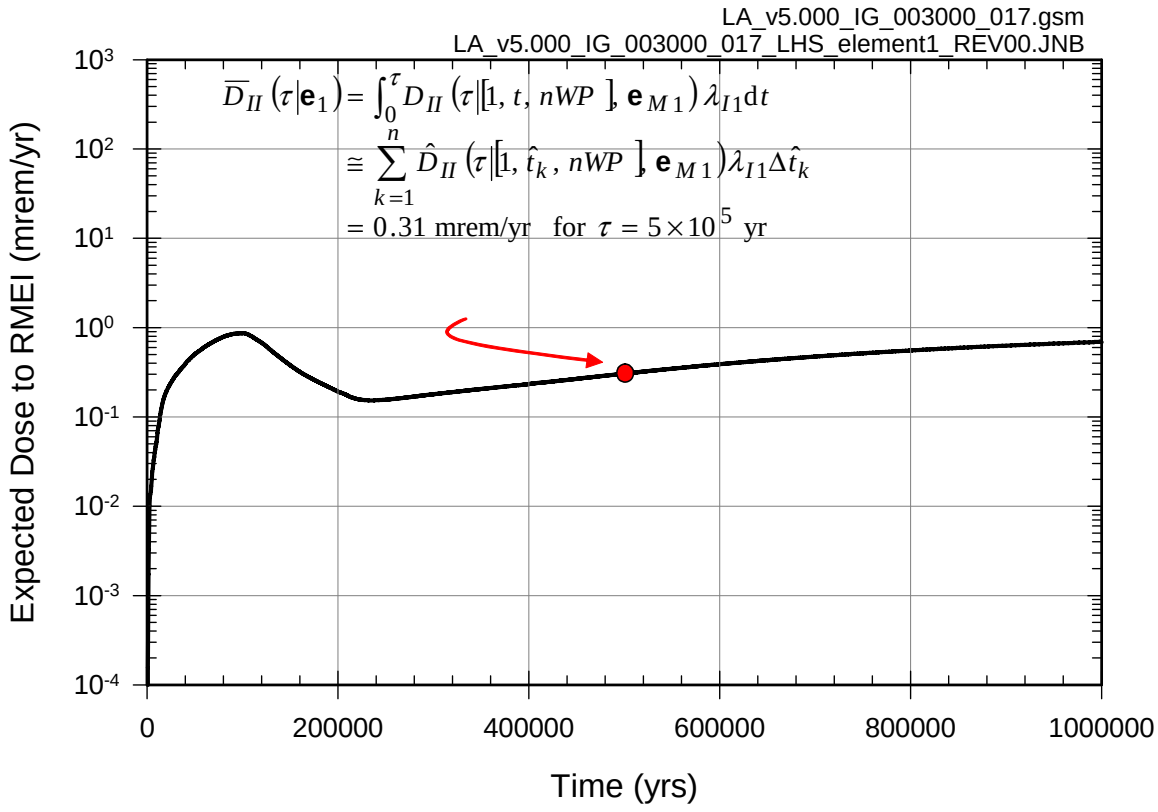

Source: Ouput DTNs: MO0709TSPAPLOT.000 [DIRS 183010]; and MO0709TSPAREGS.000 [DIRS 182976].

Figure J7.2-13. Determination of $\overline{D}_{II}(\tau|\mathbf{e}_1)$ as indicated in conjunction with Equations J7.2-7, J7.2-9 and J7.2-19 from calculated doses $D_{II}(\tau|[1, t_k, nWP], \mathbf{e}_{M1})$ shown in Equation J7.2-18 for LHS element $\mathbf{e}_1 = [\mathbf{e}_{A1}, \mathbf{e}_{M1}]$ and the time interval [0, 10^6 yr].

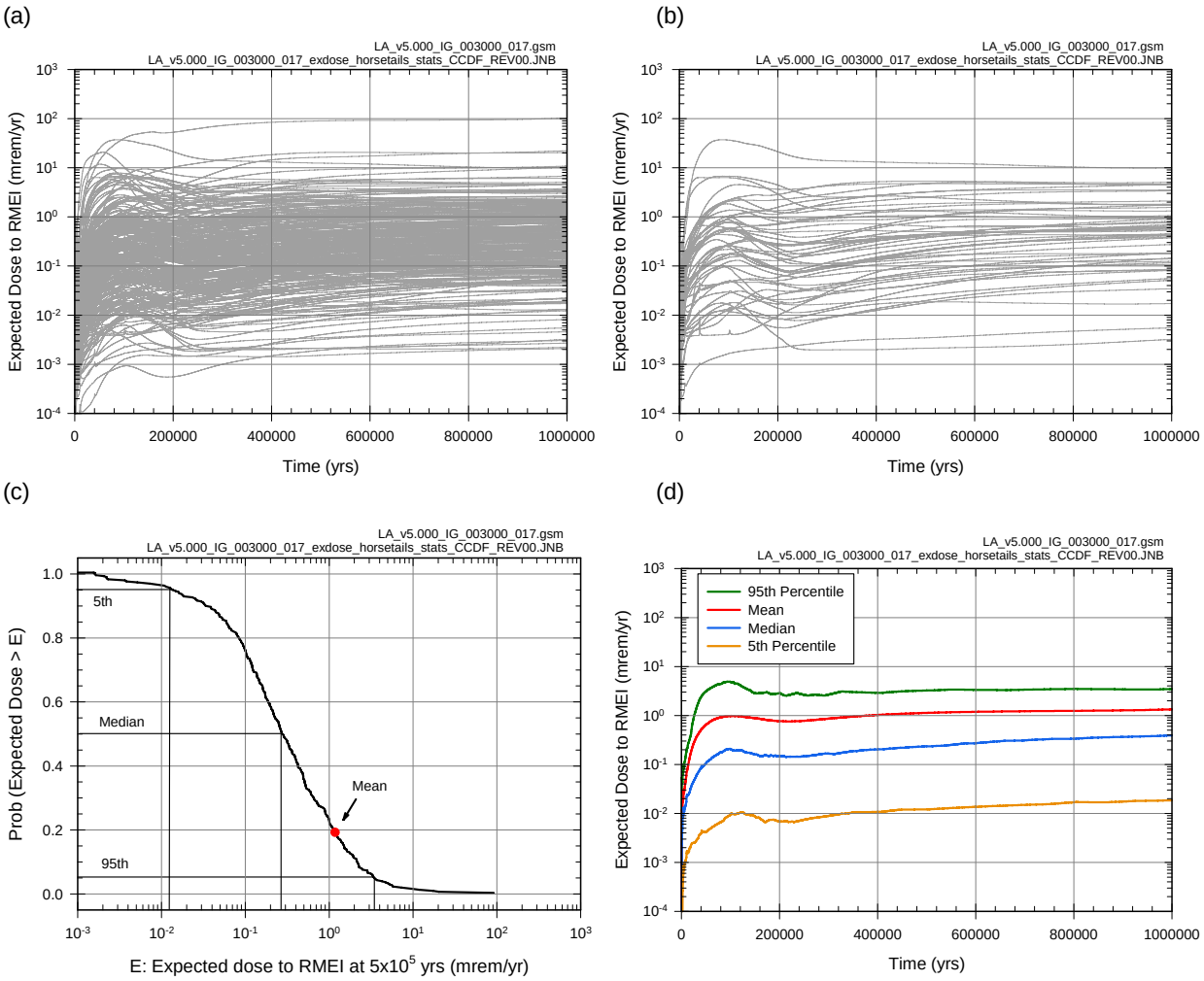

Source: Ouput DTNs: MO0709TSPAPLOT.000 [DIRS 183010]; and MO0709TSPAREGS.000 [DIRS 182976].

Figure J7.2-14. Estimate obtained with LHS of size *nLHS* = 300 showing epistemic uncertainty in expected dose $\bar{D}_{II}(\tau|\mathbf{e})$ to RMEI for $0 \le \tau \le 10^6$ yr that results when only igneous intrusion is considered: (a) expected dose $\bar{D}_{II}(\tau|\mathbf{e}_i)$, i = 1, 2, …, *nLHS* = 300, (b) expected dose $\bar{D}_{II}(\tau|\mathbf{e}_i)$, i = 1, 2, …, 50, (c) exceedance probabilities $p_E[D < \bar{D}_{II}(\tau|\mathbf{e})]$ and quantiles $Q_q[\bar{D}_{II}(\tau|\mathbf{e})]$, q = 0.05, 0.5 and 0.95, for $\tau = 5 \times 10^5$ yr, and (d) expected (mean) dose $\bar{\bar{D}}_{II}(\tau)$ and quantiles $Q_q[\bar{D}_{II}(\tau|\mathbf{e})]$, q = 0.05, 0.5, 0.95.

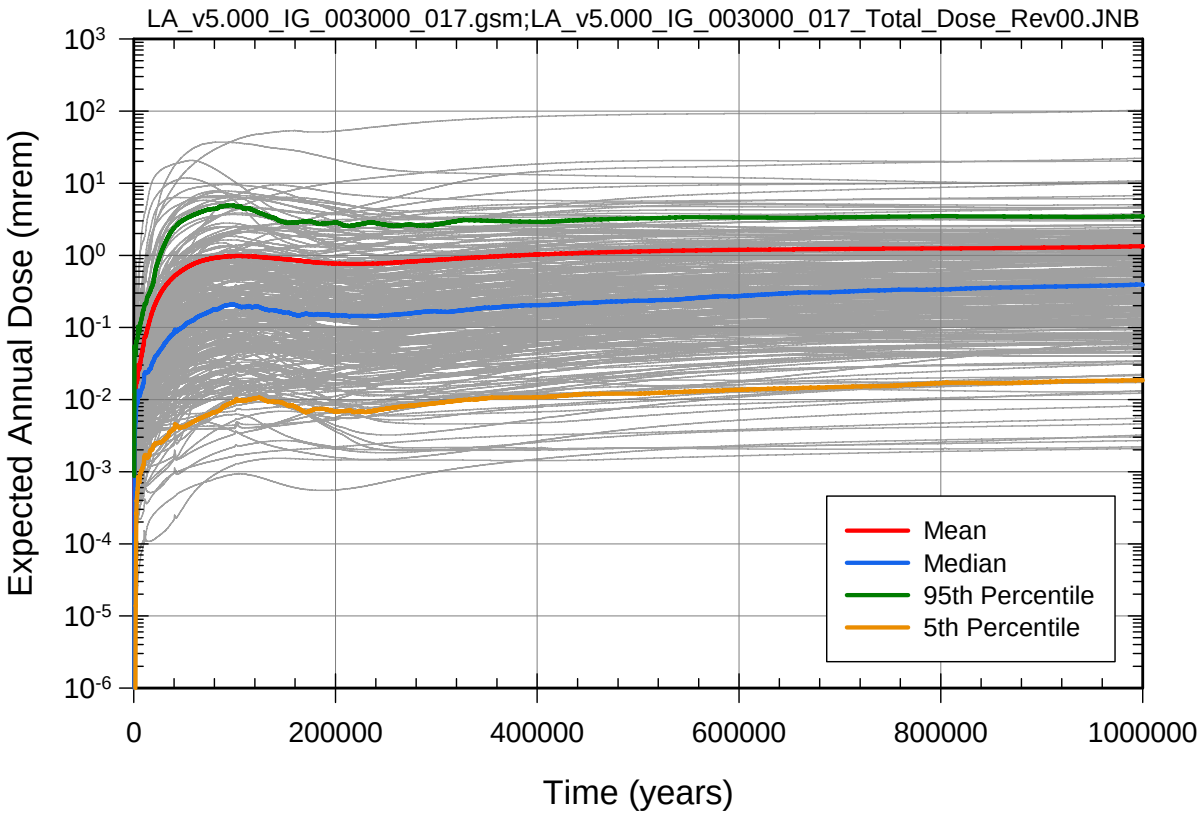

Source: Ouput DTNs: MO0709TSPAPLOT.000 [DIRS 183010]; and MO0709TSPAREGS.000 [DIRS 182976].

Figure J7.2-15. Summary presentations of epistemic uncertainty in expected dose $\bar{D}_{II}(\tau|\mathbf{e})$ to RMEI that results when only igneous intrusion is considered for $0 \leq \tau \leq 10^6$ yr.

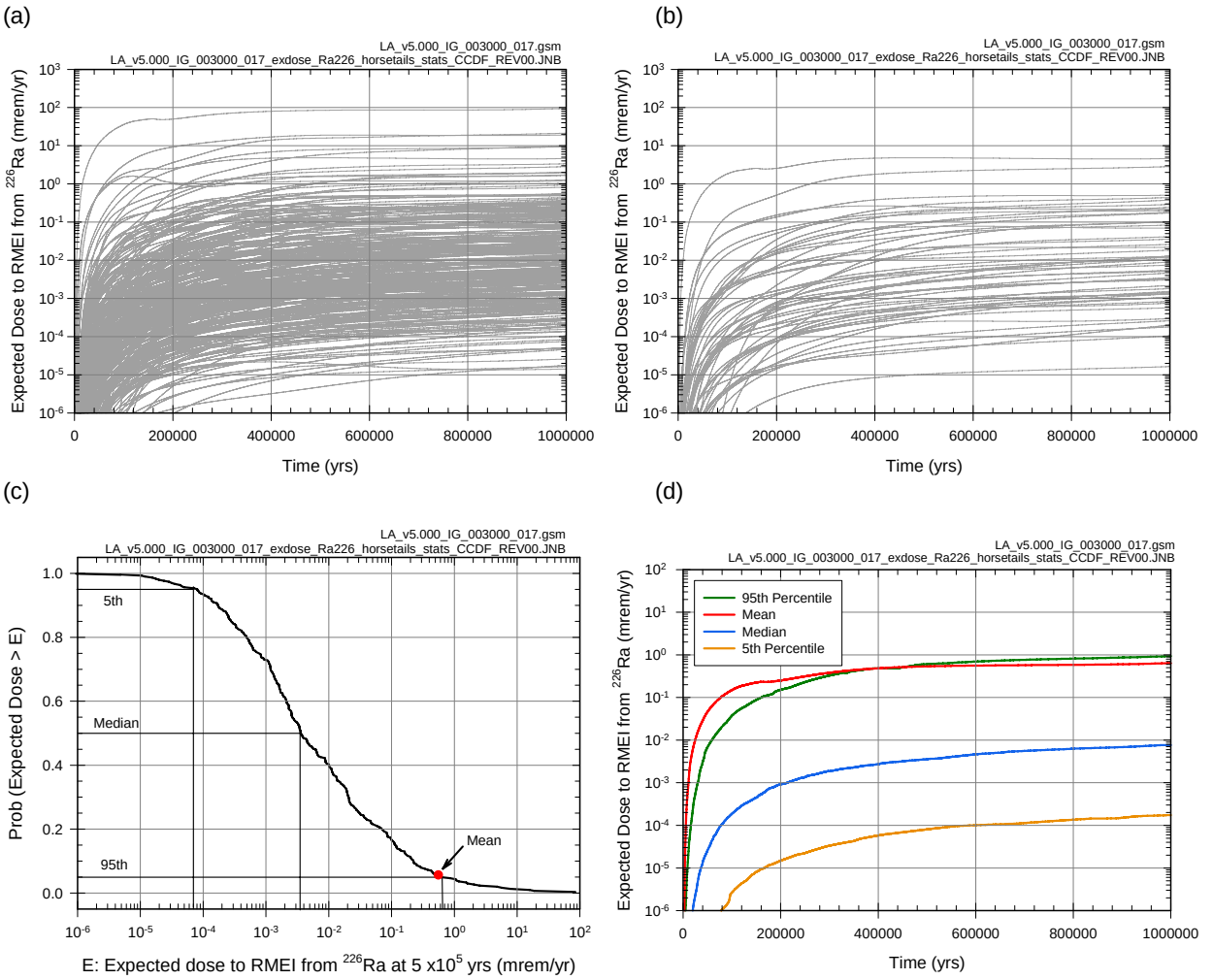

Source: Ouput DTNs: MO0709TSPAPLOT.000 [DIRS 183010]; and MO0709TSPAREGS.000 [DIRS 182976].

Figure J7.2-16. Estimate obtained with LHS of size *nLHS* = 300 showing epistemic uncertainty in expected dose $\bar{D}_{II,r}(\tau|\mathbf{e})$ to RMEI for $0 \le \tau \le 10^6$ yr with *r* corresponding to ^{226}Ra that results when only igneous intrusion is considered: (a) expected dose $\bar{D}_{II,r}(\tau|\mathbf{e}_i)$, i = 1, 2, …, *nLHS* = 300, (b) expected dose $\bar{D}_{II,r}(\tau|\mathbf{e}_i)$, i = 1, 2, …, 50, (c) exceedance probabilities $p_E[D < \bar{D}_{II,r}(\tau|\mathbf{e})]$ and quantiles $Q_q[\bar{D}_{II,r}(\tau|\mathbf{e})]$, q = 0.05, 0.5 and 0.95, for $\tau = 5 \times 10^5$ yr, and (d) expected (mean) dose $\bar{\bar{D}}_{II,r}(\tau)$ and quantiles $Q_q[\bar{D}_{II,r}(\tau|\mathbf{e})]$, q = 0.05, 0.5, 0.95.

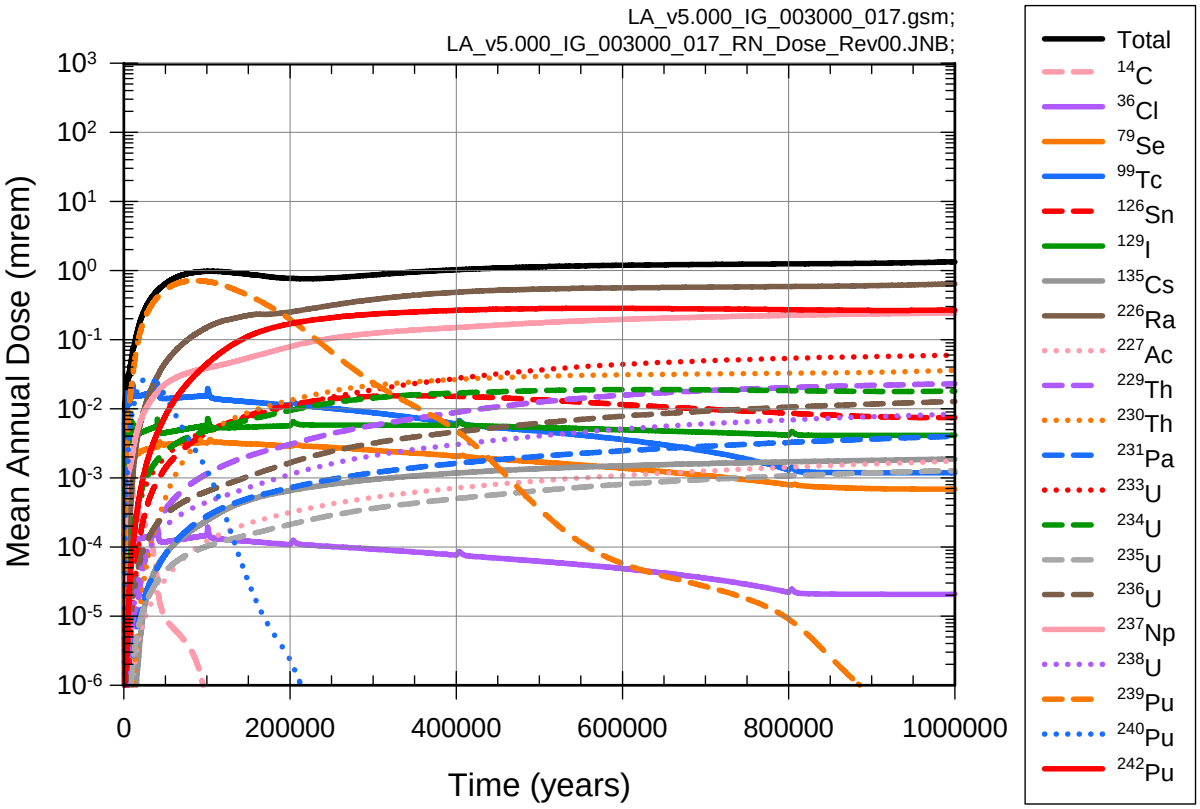

Source: Ouput DTNs: MO0709TSPAPLOT.000 [DIRS 183010]; and MO0709TSPAREGS.000 [DIRS 182976].

Figure J7.2-17. Estimates obtained with LHS of size *nLHS* = 300 of expected (mean) dose $\bar{\bar{D}}_{II,r}(\tau)$ to RMEI for $0 \leq \tau \leq 10^6$ yr for individual radioactive species that result when only igneous intrusive events are considered.

(a)

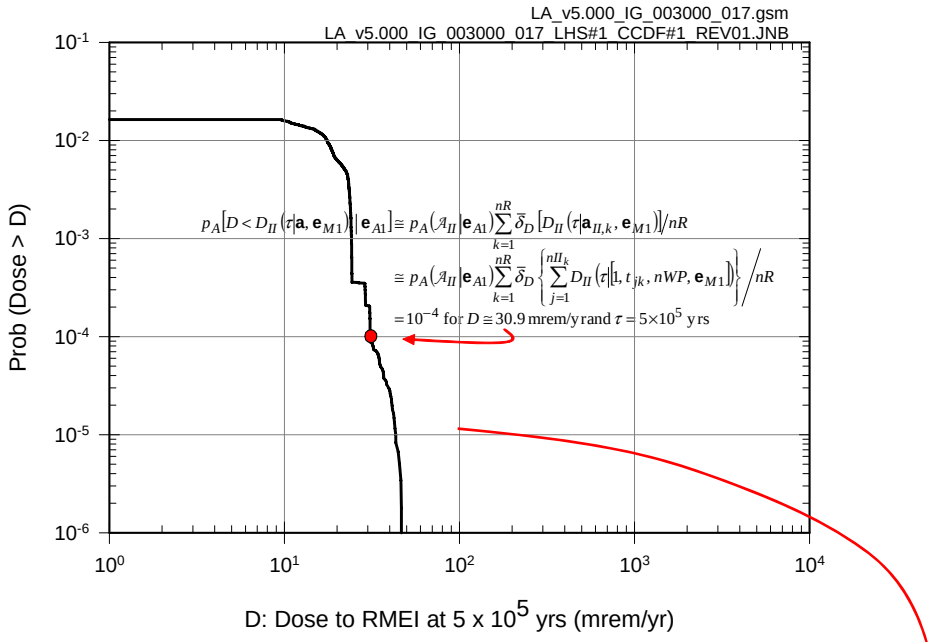

(b)

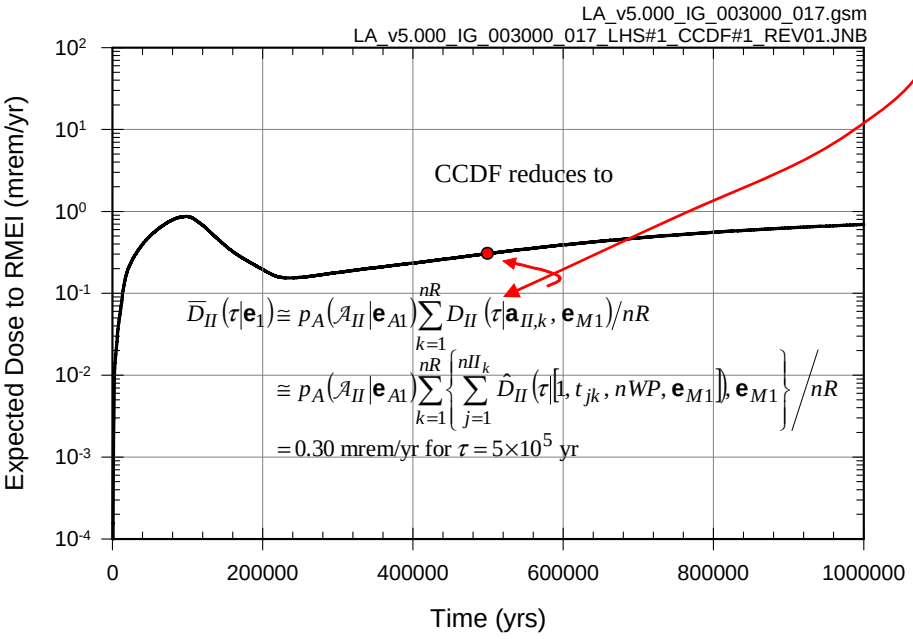

Source: Ouput DTNs: MO0709TSPAPLOT.000 [DIRS 183010]; and MO0709TSPAREGS.000 [DIRS 182976].

Figure J7.2-18. Results associated with $\bar{D}_{II}(\tau|\mathbf{e}_1)$ for LHS elements $\mathbf{e}_1 = [\mathbf{e}_{A1}, \mathbf{e}_{M1}]$ obtained with sampling-based (Monte Carlo) procedures: (a) CCDF for $D_{II}(5 \times 10^5 \text{ yr}|\mathbf{a}_{II}, \mathbf{e}_{M1})$ with exceedance probabilities $p_A[D < D_{II}(5 \times 10^5 \text{ yr}|\mathbf{a}, \mathbf{e}_{M1})|\mathbf{e}_{A1}]$ defined in Equation J7.2-23, and (b) expected dose $\bar{D}_{II}(5 \times 10^5 \text{ yr}|\mathbf{e}_1)$ associated with $D_{II}(5 \times 10^5 \text{ yr}|\mathbf{a}_{II}, \mathbf{e}_{M1})$ as defined in Equation J7.2-21.

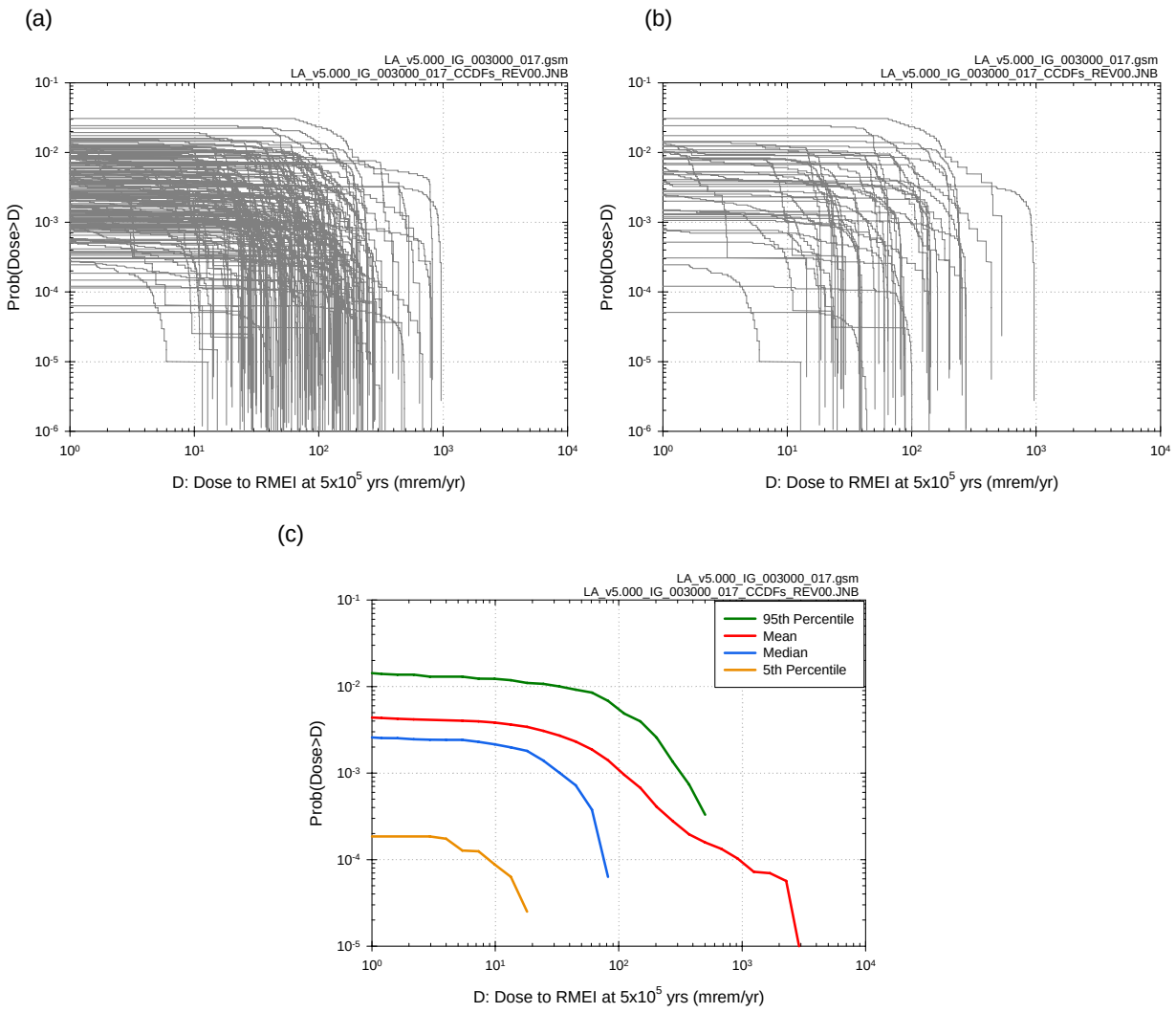

Source: Ouput DTNs: MO0709TSPAPLOT.000 [DIRS 183010]; and MO0709TSPAREGS.000 [DIRS 182976].

Figure J7.2-19. Results associated with $D_{II}(5 \times 10^5 \text{ yr}|\mathbf{a}_{II}, \mathbf{e}_M)$ obtained with sampling-based (Monte Carlo) procedures for an LHS of size $nLHS = 300$: (a) CCDFs for $D_{II}(5 \times 10^5 \text{ yr}|\mathbf{a}_{II}, \mathbf{e}_{Mi})$ with exceedance probabilities $p_A[D < D_{II}(5 \times 10^5 \text{ yr}|\mathbf{a}, \mathbf{e}_{Mi})|\mathbf{e}_{Ai}]$ defined in Equation J7.2-23 for $i = 1, 2, \ldots, nLHS = 300$, (b) CCDFs for $D_{II}(5 \times 10^5 \text{ yr}|\mathbf{a}_{II}, \mathbf{e}_{Mi})$ with exceedance probabilities $p_A[D < D_{II}(5 \times 10^5 \text{ yr}|\mathbf{a}, \mathbf{e}_{Mi})|\mathbf{a}_{Ai}]$ defined in Equation J7.2-23 for $i = 1, 2, \ldots, 50$, and (c) expected (mean) CCDF and quantile curves, $q = 0.05, 0.5, 0.95$, for CCDFs in (a).

(a)

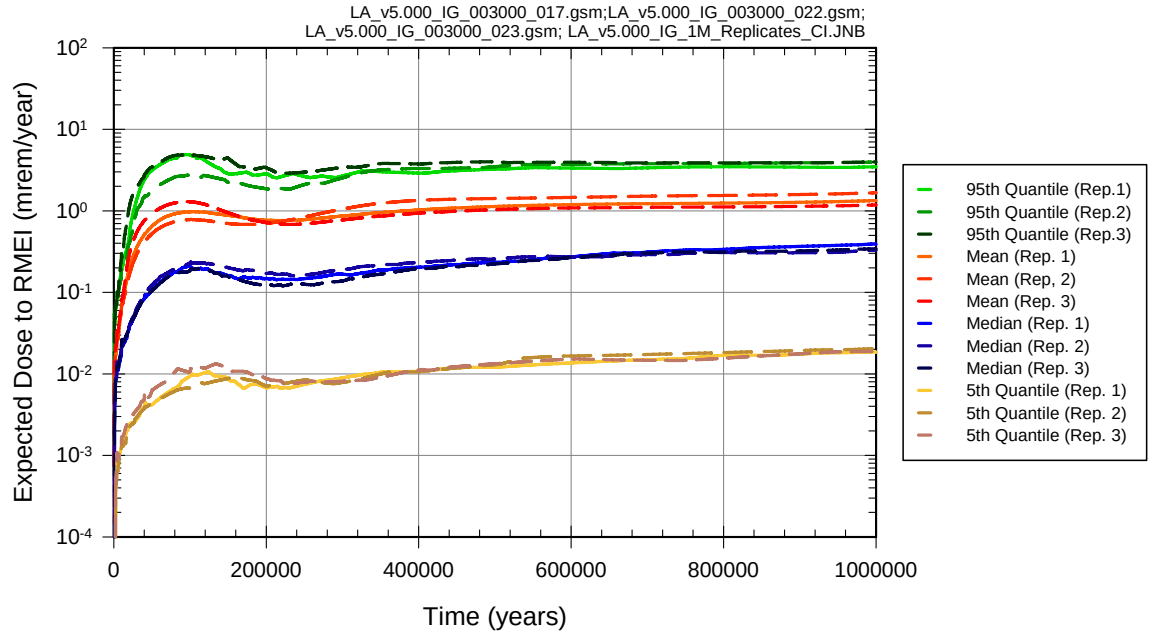

(b)

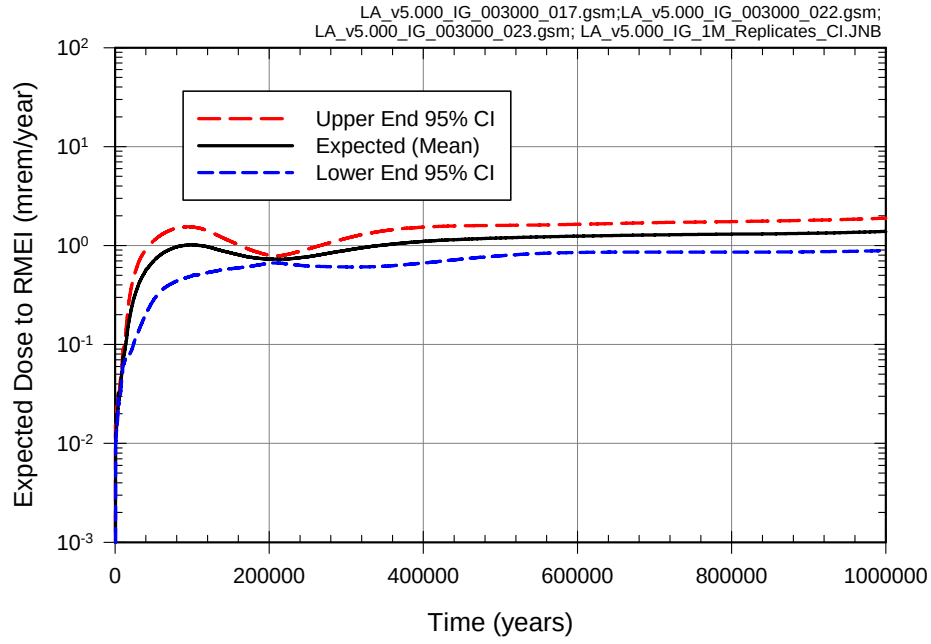

Source: Ouput DTNs: MO0709TSPAPLOT.000 [DIRS 183010]; MO0709TSPAREGS.000 [DIRS 182976]; and MO0709TSPASTAB.000 [DIRS 182983].

Figure J7.2-20. Assessment with replicated sampling of numerical error associated with use of an LHS of size *nLHS* = 300 to determine epistemic uncertainty in expected dose $\bar{D}_{II}(\tau|\mathbf{e})$ to RMEI for $0 \le \tau \le 10^6$ yr that results when only igneous intrusion is considered: (a) Replicated estimates of expected (mean) dose $\bar{\bar{D}}_{II}(\tau)$ and quantiles $Q_q[\bar{D}_{II}(\tau|\mathbf{e})]$, q = 0.05, 0.5, 0.95, and (b) confidence intervals for estimates of expected (mean) dose $\bar{\bar{D}}_{II}(\tau)$.

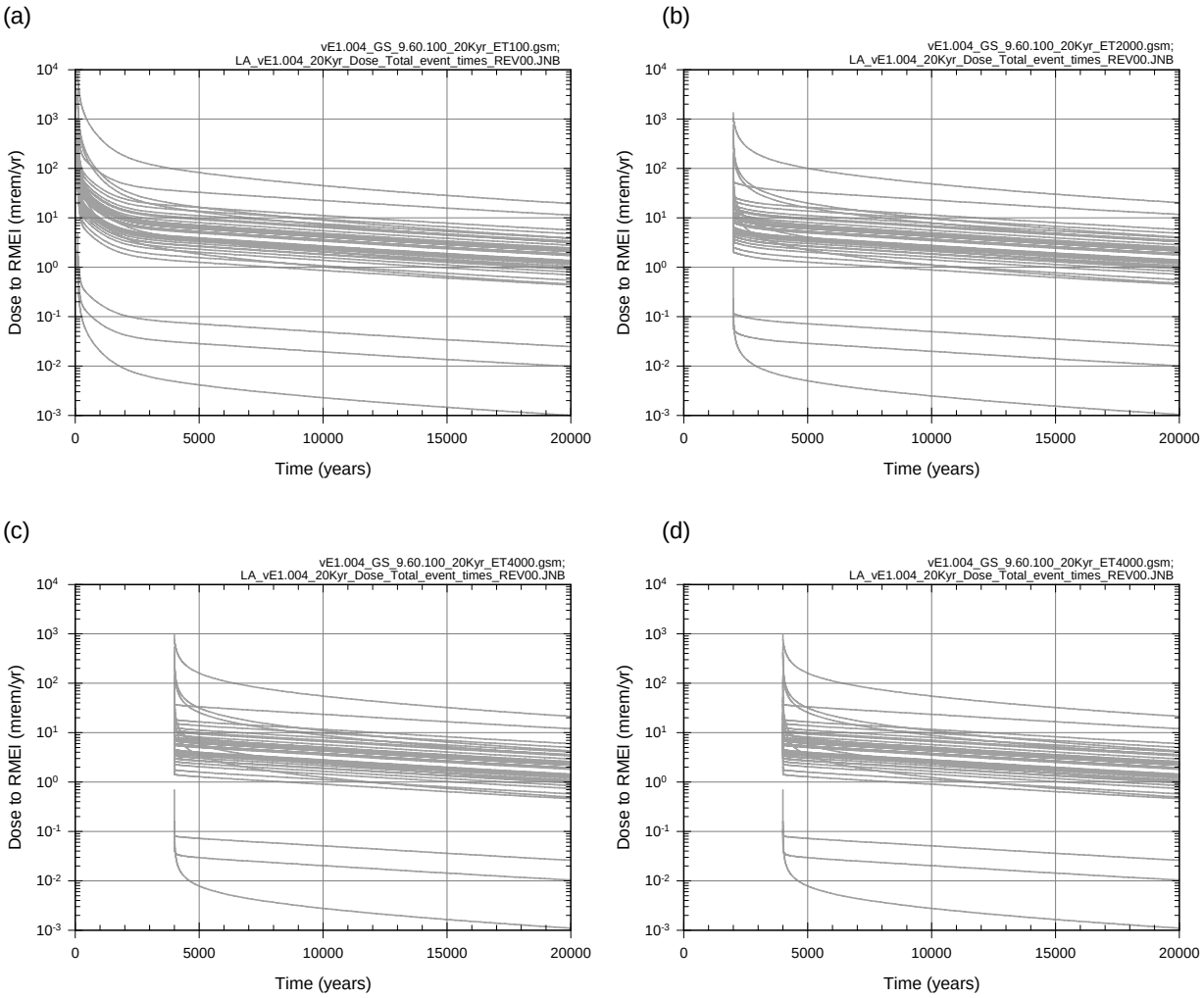

Source: Ouput DTNs: MO0709TSPAPLOT.000 [DIRS 183010]; and MO0709TSPAREGS.000 [DIRS 182976].

Figure J7.3-1. Dose results $D_{lE}(\tau|[1, t_k, 1, \mathbf{u}_l], \mathbf{e}_{M1})$ obtained for times t_k = 100, 1000, 4000, 10,000 yr, igneous eruptive properties $\mathbf{u}_l$, l = 1, 2, …, nU = 40, and LHS element $\mathbf{e}_1 = [\mathbf{e}_{A1}, \mathbf{e}_{M1}]$: (a) t_k = 100 yr, (b) t_k = 1000 yr, (c) t_k = 4000 yr, and (d) t_k = 10,000 yr.

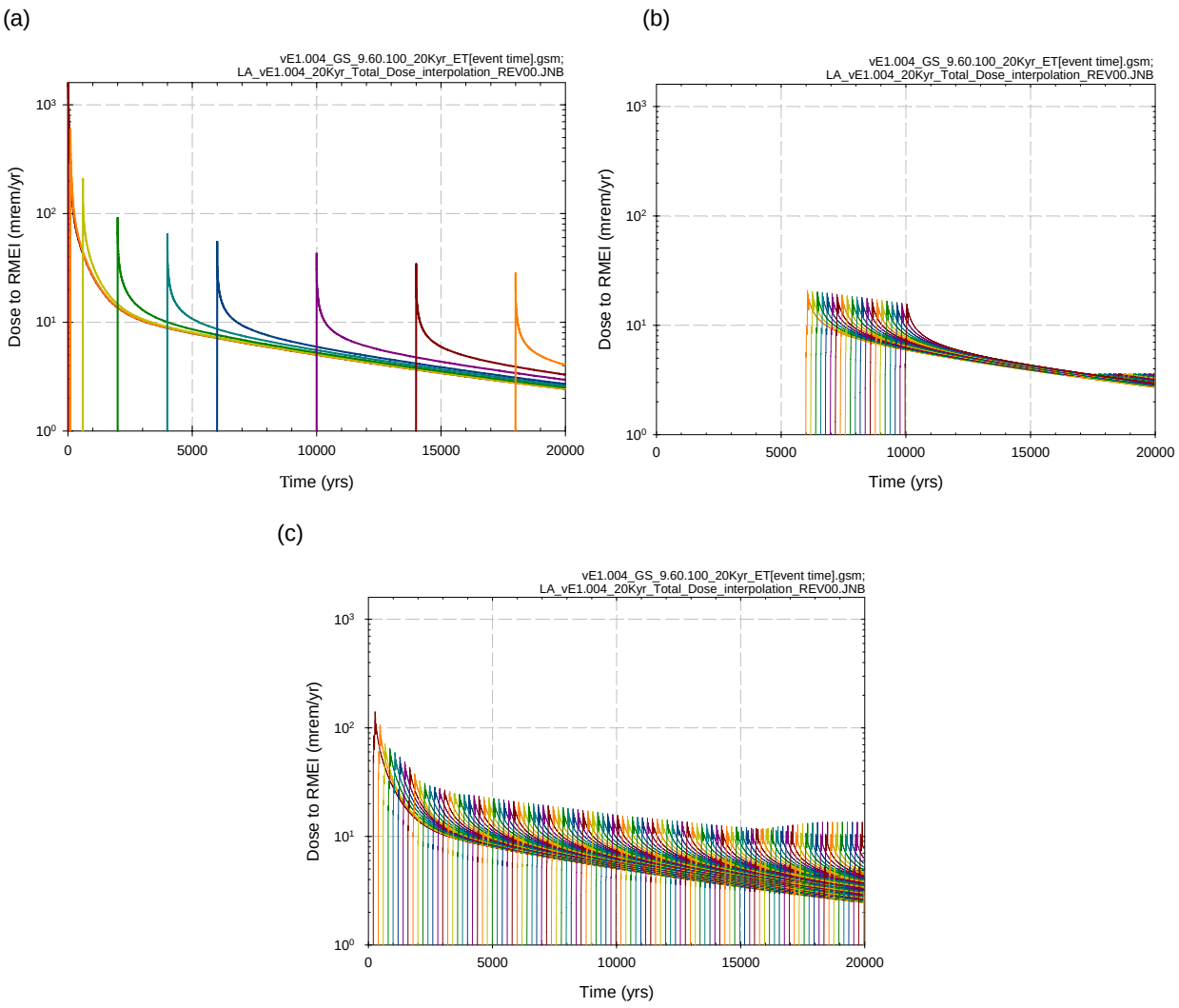

Source: Ouput DTNs: MO0709TSPAPLOT.000 [DIRS 183010]; and MO0709TSPAREGS.000 [DIRS 182976].

Figure J7.3-2. Illustration of interpolation procedure used to obtain estimates $\hat{S}(\tau|\hat{t}_k, \mathbf{e}_{M1})$ of conditional expected dose $S(\tau|t, \mathbf{e}_{M1})$ to RMEI (mrem/yr) for LHS element $\mathbf{e}_1 = [\mathbf{e}_{A1}, \mathbf{e}_{M1}]$ and the time interval [0, 20,000 yr]: (a) $S(\tau|t_k, \mathbf{e}_{M1})$, k = 1, 2, …, 10, (b) interpolated values $\hat{S}(\tau|\hat{t}_k, \mathbf{e}_{M1})$ for $\hat{t}_k$ between t_7 = 6000 yr and t_8 = 10,000 yr, and (c) interpolated values $\hat{S}(\tau|\hat{t}_k, \mathbf{e}_{M1})$ for $\hat{t}_k$ between 10 yr and 20,000 yr.

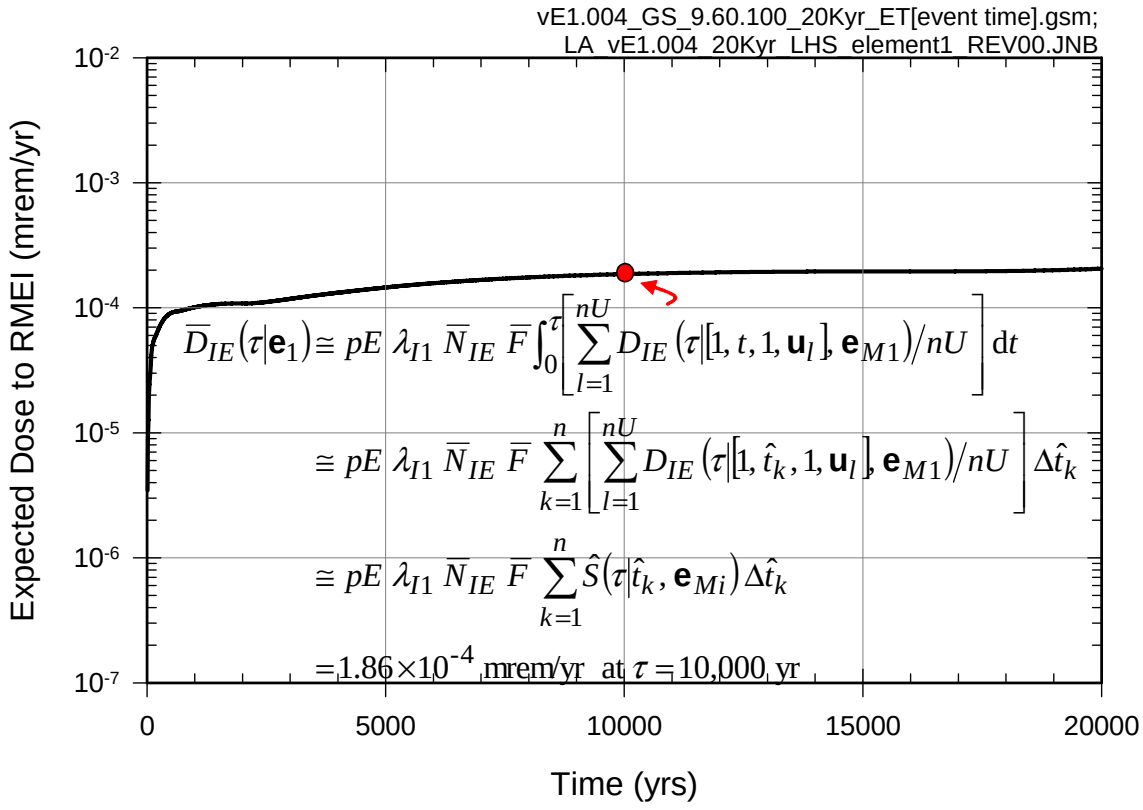

Source: Ouput DTNs: MO0709TSPAPLOT.000 [DIRS 183010]; and MO0709TSPAREGS.000 [DIRS 182976].

Figure J7.3-3. Estimate of $\bar{D}_{IE}(\tau|\ \mathbf{e}_1)$ for LHS element $\mathbf{e}_1 = [\mathbf{e}_{A1}, \mathbf{e}_{M1}]$ and $0 \le \tau \le 20{,}000$ yr with integration-based procedure indicated in Equations J7.3-9 and J7.3-16.

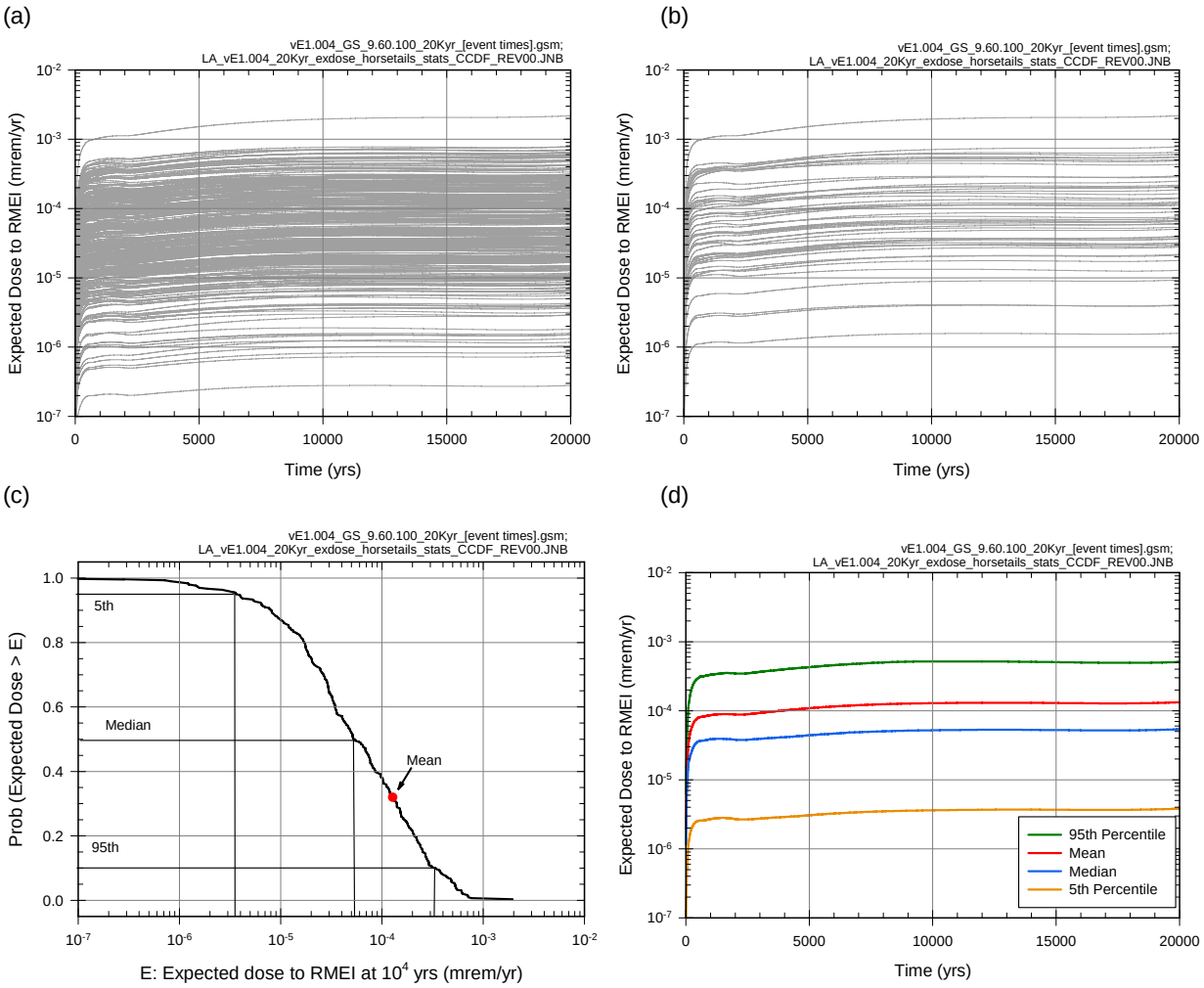

Source: Ouput DTNs: MO0709TSPAPLOT.000 [DIRS 183010]; and MO0709TSPAREGS.000 [DIRS 182976].

Figure J7.3-4. Estimate obtained with LHS of size *nLHS* = 300 showing epistemic uncertainty in expected dose $\bar{D}_{IE}(\tau|\mathbf{e})$ to RMEI for $0 \le \tau \le 20{,}000$ yr that results when only igneous eruptive events are considered: (a) expected dose $\bar{D}_{IE}(\tau|\mathbf{e}_i)$, $i = 1, 2, \ldots, nLHS = 300$, (b) expected dose $\bar{D}_{IE}(\tau|\mathbf{e}_i)$, $i = 1, 2, \ldots, 50$, (c) exceedance probabilities $p_E[D < \bar{D}_{IE}(\tau|\mathbf{e})]$ and quantiles $Q_q[\bar{D}_{IE}(\tau|\mathbf{e})]$, $q = 0.05$, 0.5 and 0.95, for $\tau = 10^4$ yr, and (d) expected (mean) dose $\bar{\bar{D}}_{IE}(\tau)$ and quantiles $Q_q[\bar{D}_{IE}(\tau|\mathbf{e})]$, $q = 0.05$, 0.5, 0.95.

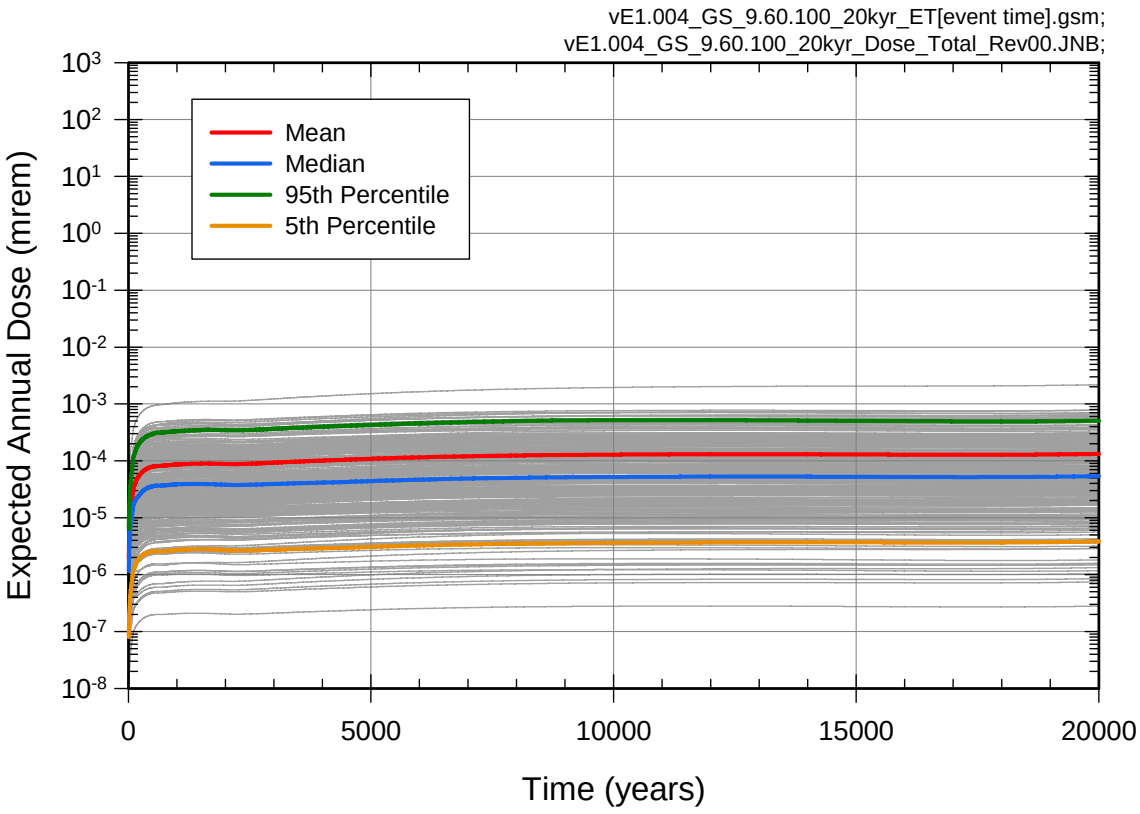

Source: Ouput DTNs: MO0709TSPAPLOT.000 [DIRS 183010]; and MO0709TSPAREGS.000 [DIRS 182976].

Figure J7.3-5. Summary of results obtained with LHS of size *nLHS* = 300 showing epistemic uncertainty in expected dose $\bar{D}_{IE}(\tau|\mathbf{e})$ to RMEI for $0 \leq \tau \leq 20{,}000$ yr that results when only igneous eruptive events are considered.

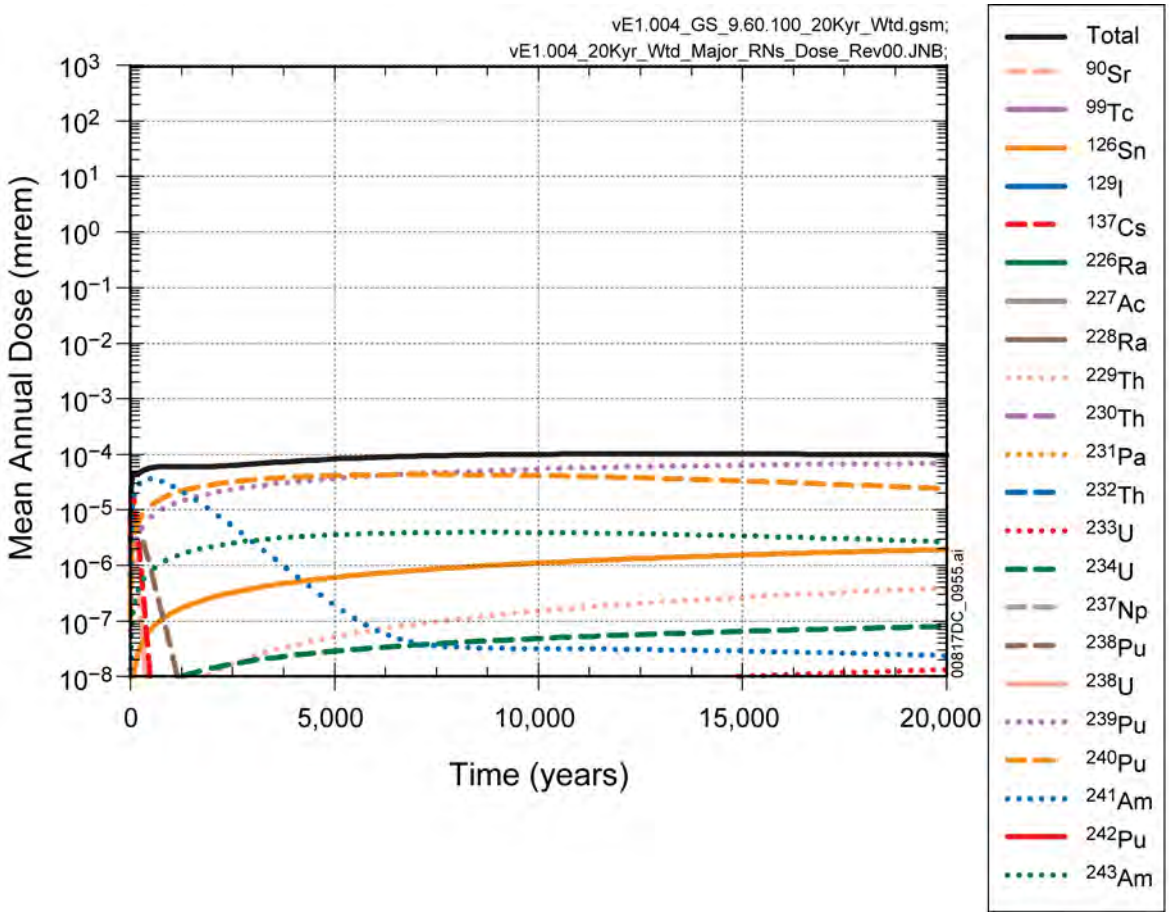

Source: Ouput DTNs: MO0709TSPAPLOT.000 [DIRS 183010]; and MO0709TSPAREGS.000 [DIRS 182976].

Figure J7.3-6. Estimates obtained with LHS of size *nLHS* = 300 of expected (mean) dose $\bar{\bar{D}}_{IE,r}(\tau)$ to RMEI for $0 \leq \tau \leq 20{,}000$ yr for individual radioactive species that result when only igneous eruptive events are considered.

(a)

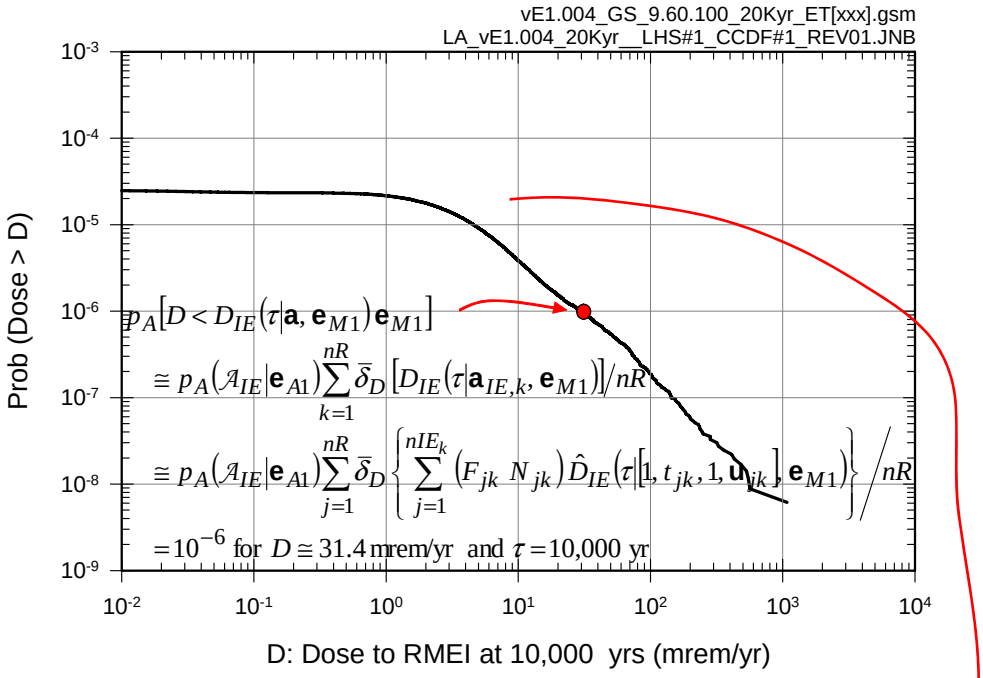

(b)

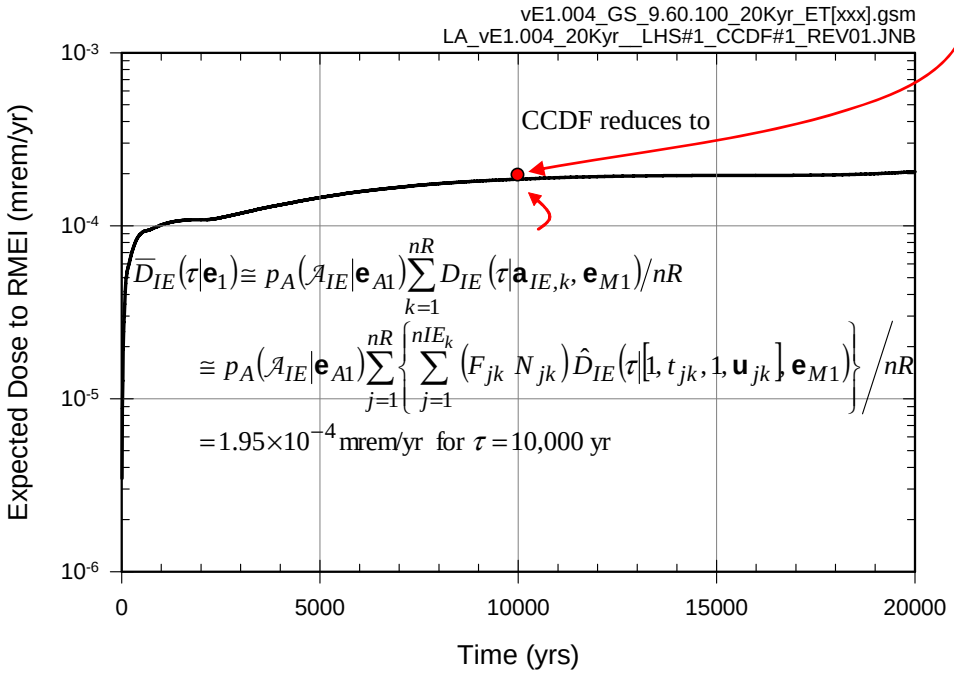

Source: Ouput DTNs: MO0709TSPAPLOT.000 [DIRS 183010]; and MO0709TSPAREGS.000 [DIRS 182976].

Figure J7.3-7. Results associated with $D_{IE}(\tau|\mathbf{a}_{IE}, \mathbf{e}_1)$ for LHS element $\mathbf{e}_1 = [\mathbf{e}_{A1}, \mathbf{e}_{M1}]$ obtained with sampling-based (Monte Carlo) procedures: (a) CCDF for $D_{IE}(10^4 \text{ yr}|\mathbf{a}_{IE}, \mathbf{e}_1)$ with exceedance probabilities $p_A[D < D_{IE}(10^4 \text{ yr}|\mathbf{a}, \mathbf{e}_{M1})|\mathbf{e}_{A1}]$ defined in Equation J7.3-20, and (b) expected dose $\bar{D}_{IE}(10^4 \text{ yr}|\mathbf{e}_1)$ associated with $D_{IE}(10^4 \text{ yr}|\mathbf{a}_{IE}, \mathbf{e}_1)$ as defined in Equation J7.3-18.

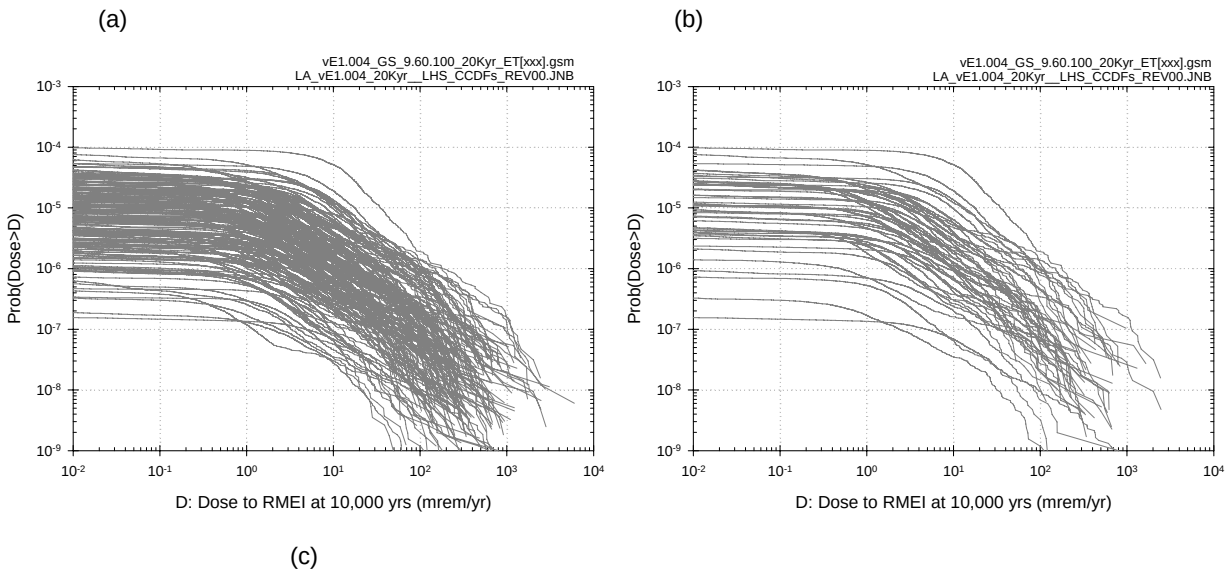

Source: Ouput DTNs: MO0709TSPAPLOT.000 [DIRS 183010]; and MO0709TSPAREGS.000 [DIRS 182976].

Figure J7.3-8. Results associated with $D_{IE}(10^4 \text{ yr}|\mathbf{a}_{IE}, e_M)$ obtained with sampling-based (Monte Carlo) procedures for an LHS of size $nLHS = 300$: (a) CCDFs for $D_{IE}(10^4 \text{ yr}|\mathbf{e}_{IE}, e_{Mi})$ with exceedance probabilities $p_A[D < D_{IE}(10^4 \text{ yr}|\mathbf{a}, \mathbf{e}_{Mi})|\mathbf{e}_{Ai}]$ defined in Equation J7.3-20 for $i = 1, 2, \ldots, nLHS = 300$, (b) CCDFs for $D_{IE}(10^4 \text{ yr}|\mathbf{a}_{IE}, e_{Mi})$ with exceedance probabilities $p_A[D < D_{IE}(10^4 \text{ yr}|\mathbf{a}, \mathbf{e}_{Mi})|\mathbf{e}_{Ai}]$ defined in Equation J7.3-20 for $i = 1, 2, \ldots, 50$, and (c) expected (mean) CCDF and quantile curves, $q = 0.05, 0.5, 0.95$, for CCDFs in (a).

(a)

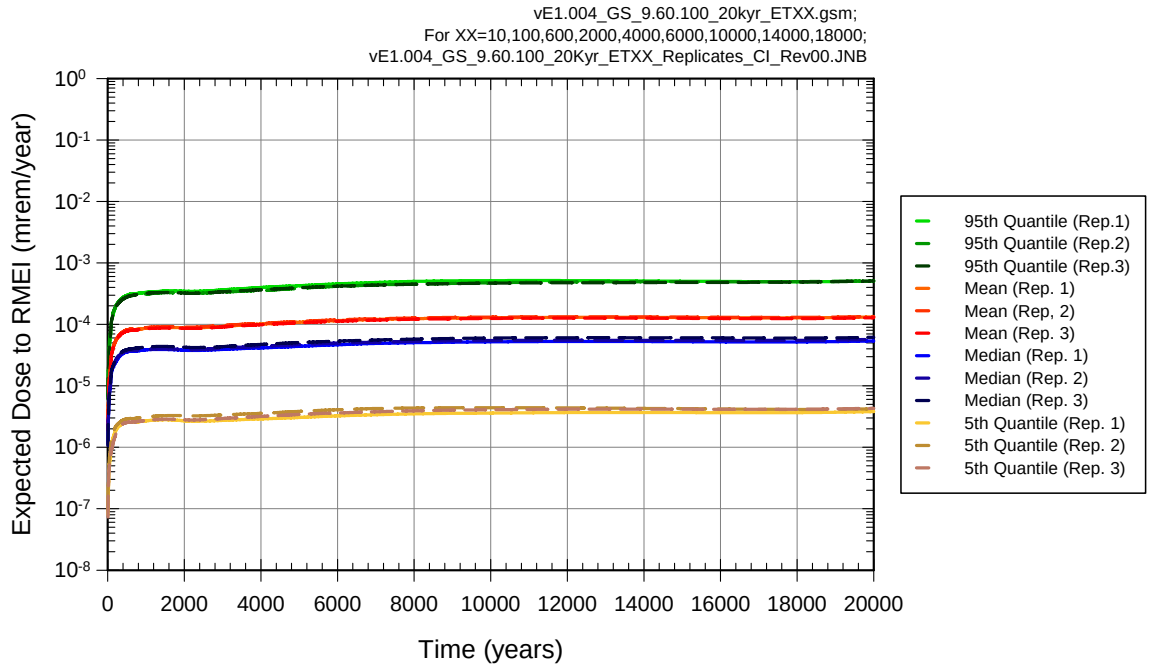

(b)

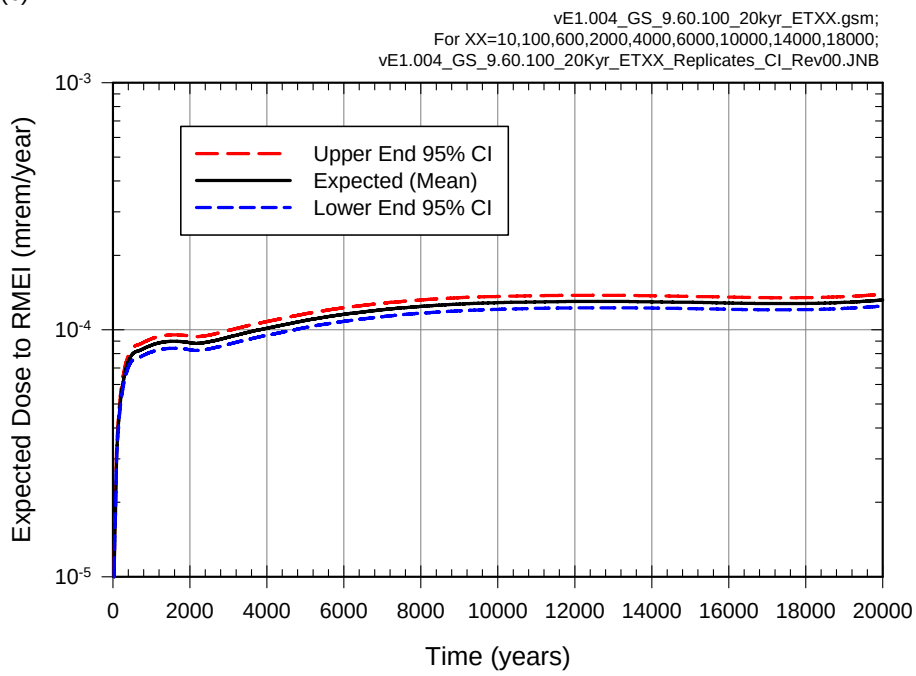

Source: Ouput DTNs: MO0709TSPAPLOT.000 [DIRS 183010]; and MO0709TSPAREGS.000 [DIRS 182976].

Figure J7.3-9. Assessment with replicated sampling of numerical error associated with use of an LHS of size *nLHS* = 300 to determine epistemic uncertainty in expected dose $\bar{D}_{IE}(\tau)$ to RMEI for $0 \leq \tau \leq 20{,}000$ yr that results when only igneous eruptive events are considered: (a) Replicated estimates of expected (mean) dose $\bar{D}_{IE}(\tau)$ and quantiles $Q_q[\bar{D}_{IE}(\tau|\mathbf{e})]$, q = 0.05, 0.5, 0.95, and (b) confidence intervals for estimates of expected (mean) dose $\bar{\bar{D}}_{IE}(\tau)$.

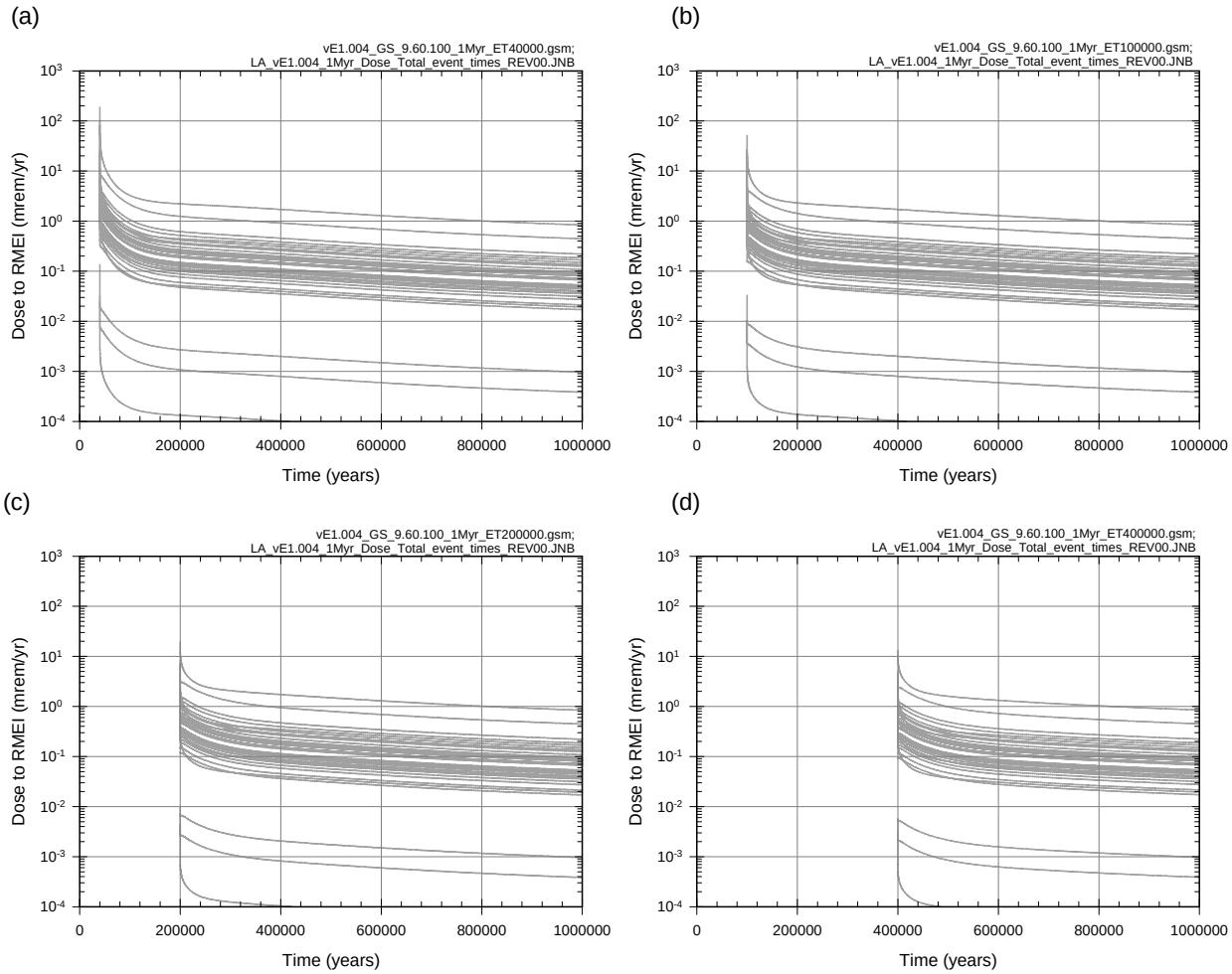

Source: Ouput DTNs: MO0709TSPAPLOT.000 [DIRS 183010]; and MO0709TSPAREGS.000 [DIRS 182976].

Figure J7.3-10. Dose results $D_{IE}(\tau|[1, t_k, 1, \mathbf{u}_l], \mathbf{e}_{M1})$ obtained for times t_k = 40,000, 100,000, 200,000, 400,000 yr, igneous eruptive properties $\mathbf{u}_l$, l = 1, 2, …, nU = 40, and LHS element $\mathbf{e}_1 = [\mathbf{e}_{A1}, \mathbf{e}_{M1}]$: (a) t_k = 40,000 yr, (b) t_k = 100,000 yr, (c) t_k = 200,000 yr, and (d) t_k = 400,000 yr.

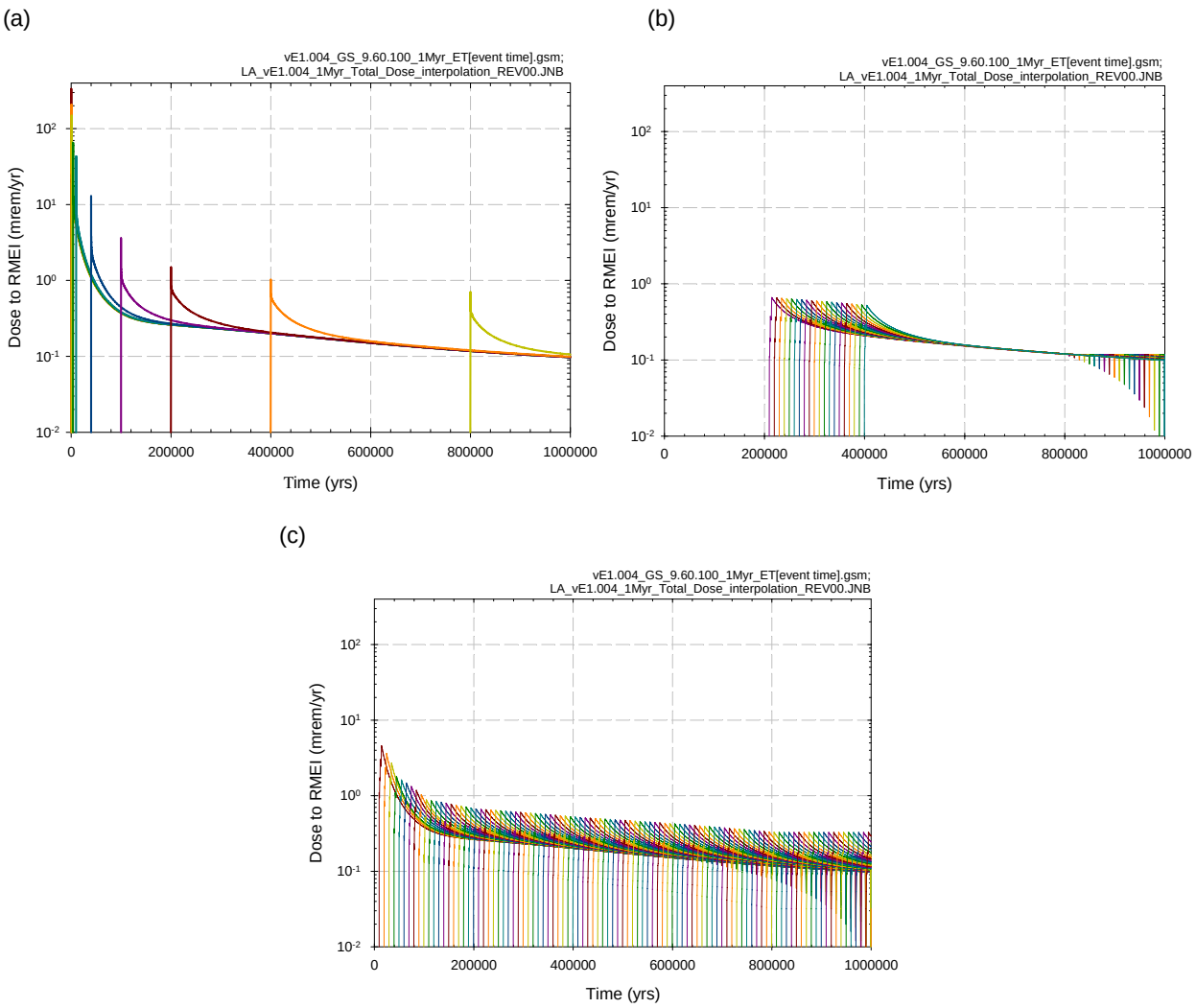

Source: Ouput DTNs: MO0709TSPAPLOT.000 [DIRS 183010]; and MO0709TSPAREGS.000 [DIRS 182976].

Figure J7.3-11. Illustration of interpolation procedure used to obtain estimates $\hat{S}(\tau|\hat{t}_k, \mathbf{e}_{Mi})$ of conditional expected dose $S(\tau|t, \mathbf{e}_{M1})$ to RMEI (mrem/yr) for LHS element $\mathbf{e}_1 = [\mathbf{e}_{A1}, \mathbf{e}_{M1}]$ and the time interval [0, 10^6 yr]: (a) $S(\tau|t_k, \mathbf{e}_{M1})$, k = 1, 2, …, 10, (b) interpolated values $\hat{S}(\tau|\hat{t}_k, \mathbf{e}_{M1})$ for $\hat{t}_k$ between t_8 = 200,000 yr and t_9 = 400,000 yr, and (c) interpolated values $\hat{S}(\tau|\hat{t}_k, \mathbf{e}_{M1})$ for $\hat{t}_k$ between 250 yr and 10^6 yr.

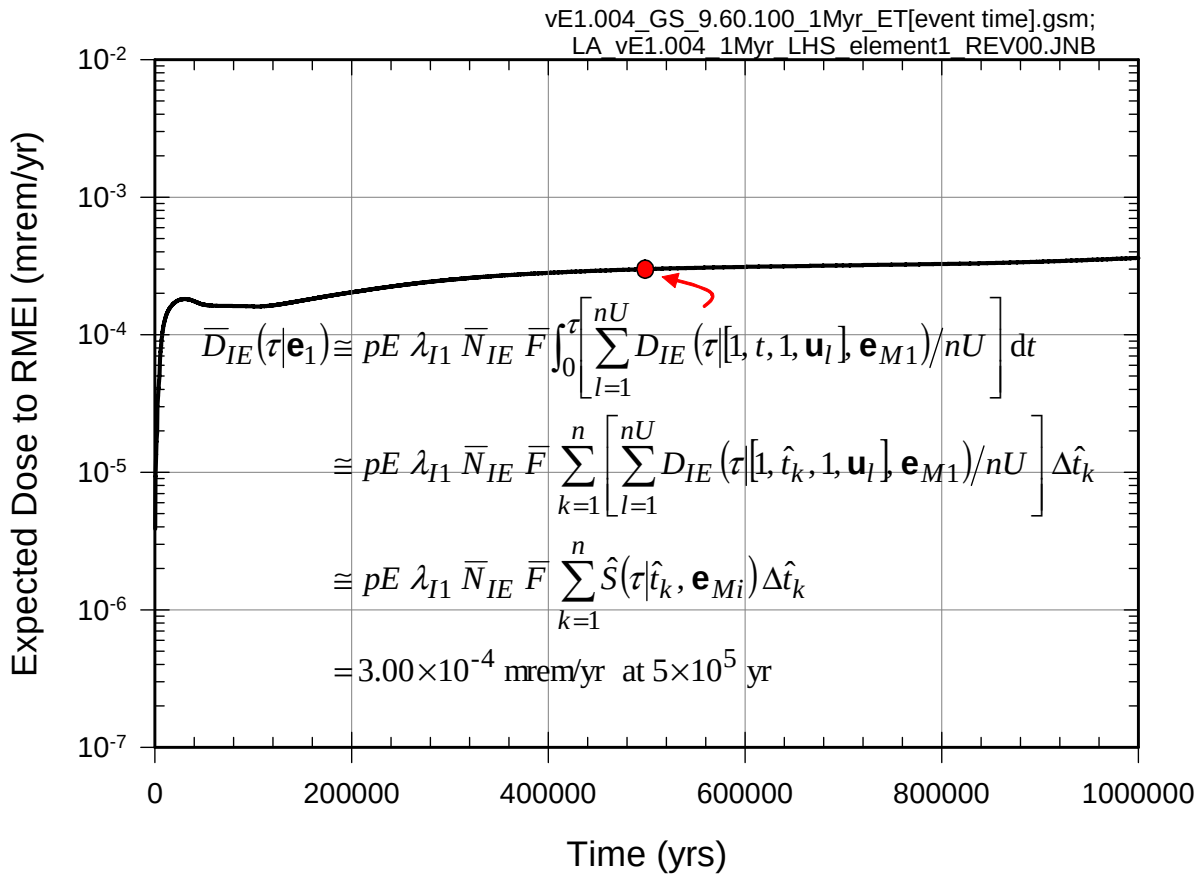

Source: Ouput DTNs: MO0709TSPAPLOT.000 [DIRS 183010]; and MO0709TSPAREGS.000 [DIRS 182976].

Figure J7.3-12. Estimate of $\overline{D}_{IE}(\tau|\mathbf{e}_1)$ for LHS element $\mathbf{e}_1 = [\mathbf{e}_{A1}, \mathbf{e}_{M1}]$ and $0 \le \tau \le 10^6$ yr with integration-based procedure indicated in Equations J7.3-9 and J7.3-16.

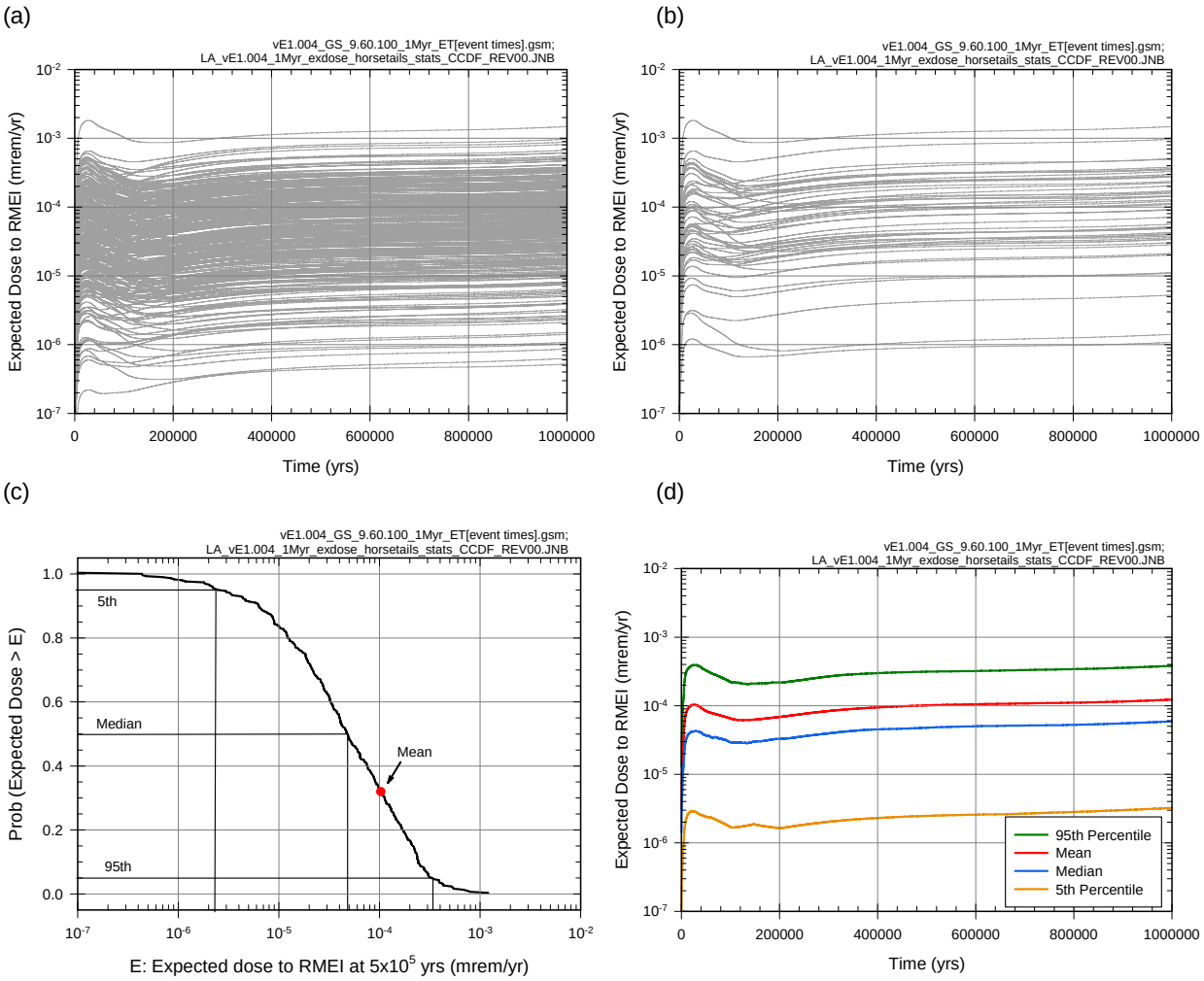

Source: Ouput DTNs: MO0709TSPAPLOT.000 [DIRS 183010]; and MO0709TSPAREGS.000 [DIRS 182976].

Figure J7.3-13. Estimate obtained with LHS of size *nLHS* = 300 showing epistemic uncertainty in expected dose $\bar{D}_{IE}(\tau|\mathbf{e})$ to RMEI for $0 \le \tau \le 10^6$ yr that results when only igneous eruptive events are considered: (a) expected dose $\bar{D}_{IE}(\tau|\mathbf{e}_i)$, i = 1, 2, …, *nLHS* = 300, (b) expected dose $\bar{D}_{IE}(\tau|\mathbf{e}_i)$, i = 1, 2, …, 50, (c) exceedance probabilities $p_E[D < \bar{D}_{IE}(\tau|\mathbf{e})]$ and quantiles $Q_q[\bar{D}_{IE}(\tau|\mathbf{e})]$, q = 0.05, 0.5 and 0.95, for τ = 500,000 yr, and (d) expected (mean) dose $\bar{\bar{D}}_{IE}(\tau)$ and quantiles $Q_q[\bar{D}_{IE}(\tau|\mathbf{e})]$, q = 0.05, 0.5, 0.95.

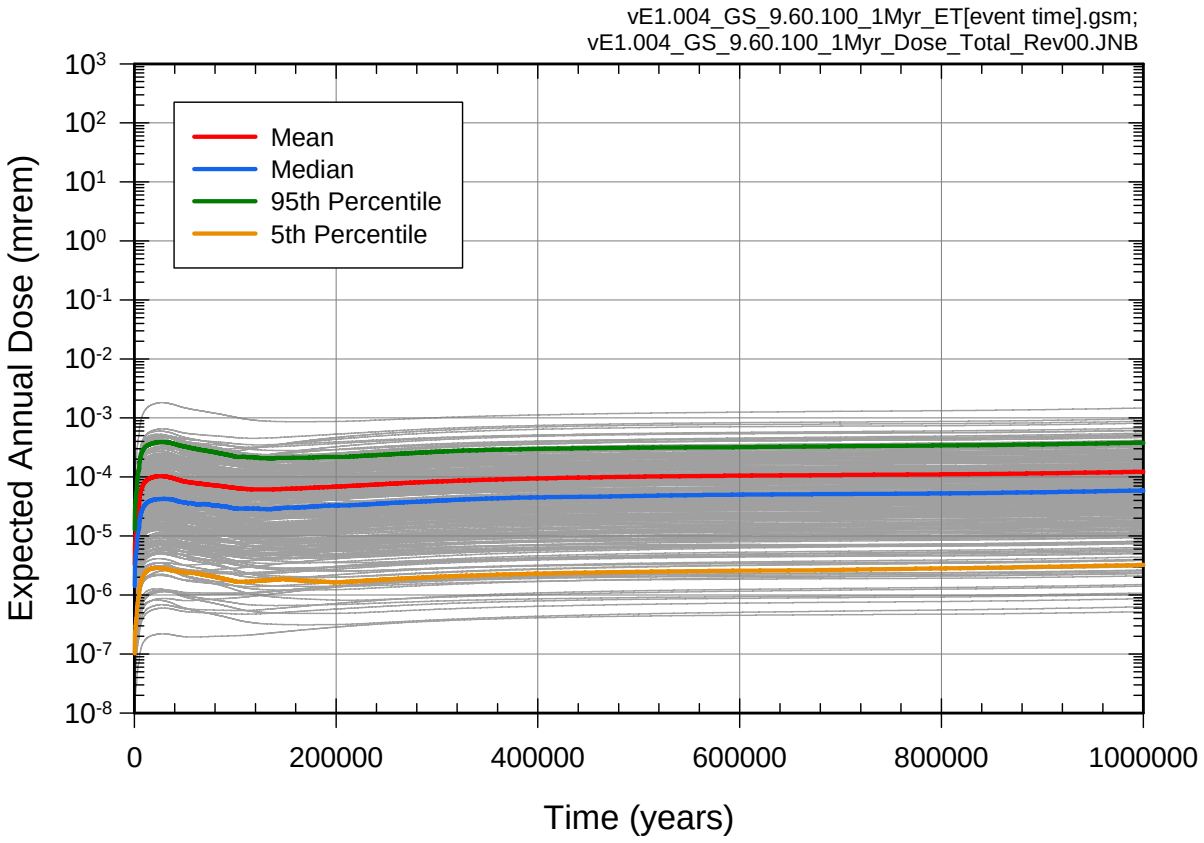

Source: Ouput DTNs: MO0709TSPAPLOT.000 [DIRS 183010]; and MO0709TSPAREGS.000 [DIRS 182976].

Figure J7.3-14. Summary of results obtained with LHS of size *nLHS* = 300 showing epistemic uncertainty in expected dose $\bar{D}_{IE}(\tau|\mathbf{e})$ to RMEI for $0 \le \tau \le 10^6$ yr that results when only igneous eruptive events are considered.

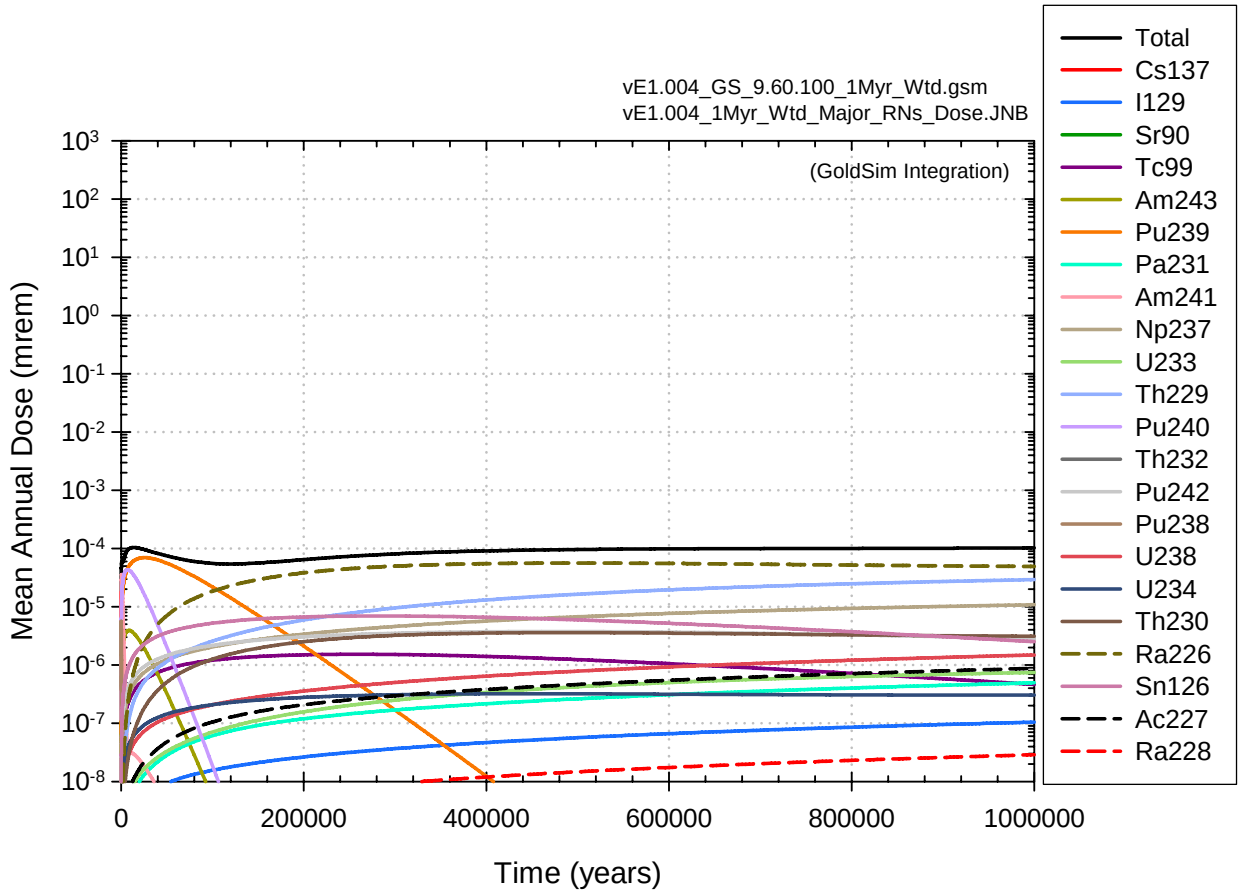

Source: Ouput DTNs: MO0709TSPAPLOT.000 [DIRS 183010]; and MO0709TSPAREGS.000 [DIRS 182976].

Figure J7.3-15. Estimates obtained with LHS of size *nLHS* = 300 of expected (mean) dose $\bar{\bar{D}}_{IE,r}(\tau)$ to RMEI for $0 \leq \tau \leq 10^6$ yr for individual radioactive species that result when only igneous eruptive events are considered.

(a)

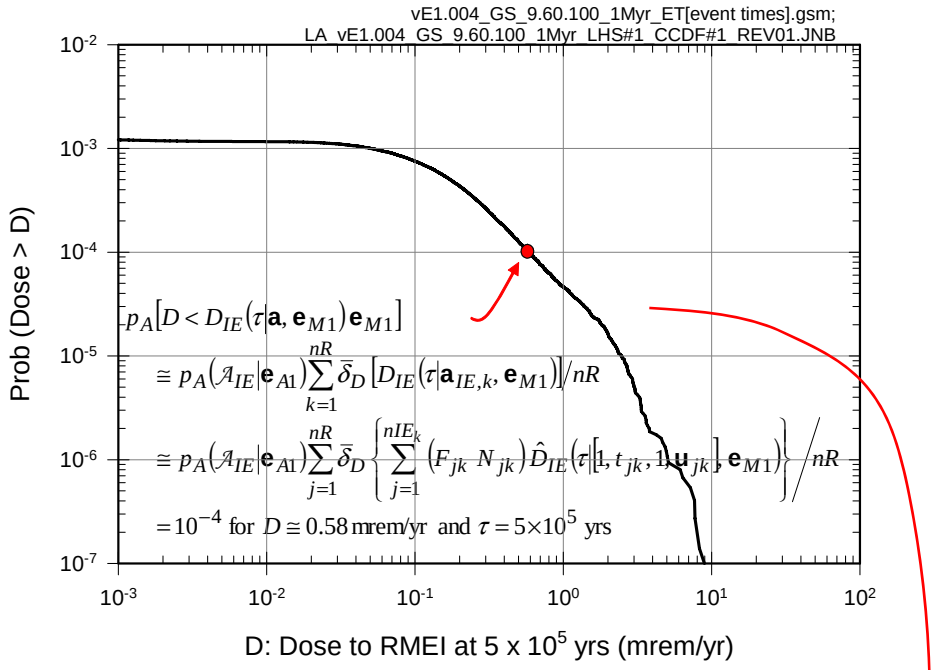

(b)

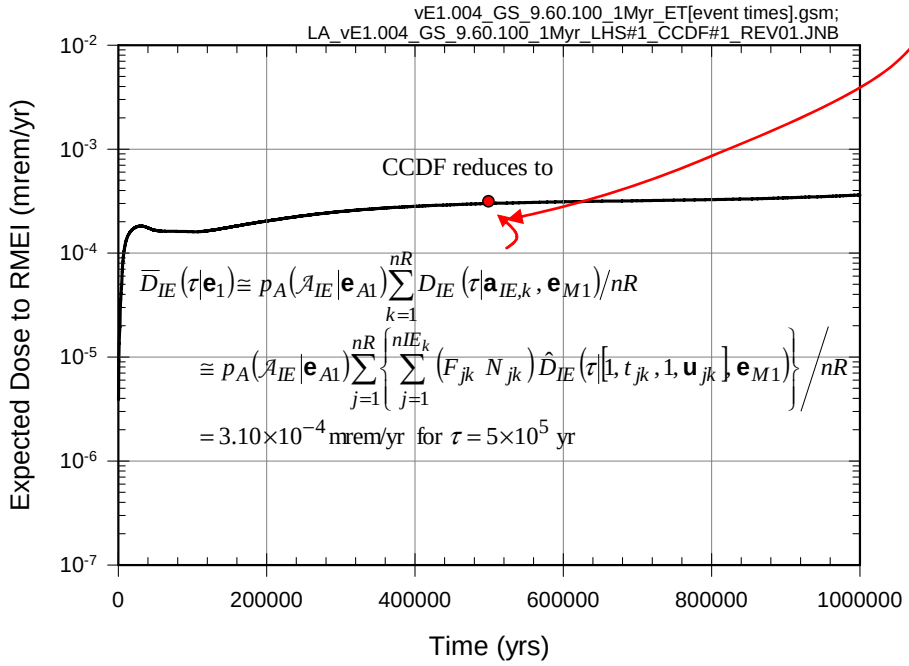

Source: Ouput DTNs: MO0709TSPAPLOT.000 [DIRS 183010]; and MO0709TSPAREGS.000 [DIRS 182976].

Figure J7.3-16. Results associated with $D_{IE}(\tau|\mathbf{a}_{IE}, \mathbf{e}_{M1})$ for LHS element $\mathbf{e}_1 = [\mathbf{e}_{A1}, \mathbf{e}_{M1}]$ obtained with sampling-based (Monte Carlo) procedures: (a) CCDF for $D_{IE}(500{,}000\ \text{yr}|\mathbf{a}_{IE}, \mathbf{e}_{M1})$ with exceedance probabilities $p_A[D < D_{IE}(500{,}000\ \text{yr}|\mathbf{a}, \mathbf{e}_{M1})|\mathbf{e}_{A1}]$ defined in Equation J7.3-20, and (b) expected dose $\bar{D}_{IE}(500{,}000\ \text{yr}|\mathbf{e}_1)$ associated with $D_{IE}(500{,}000\ \text{yr}|\mathbf{a}_{IE}, \mathbf{e}_{M1})$ as defined in Equation J7.3-18.

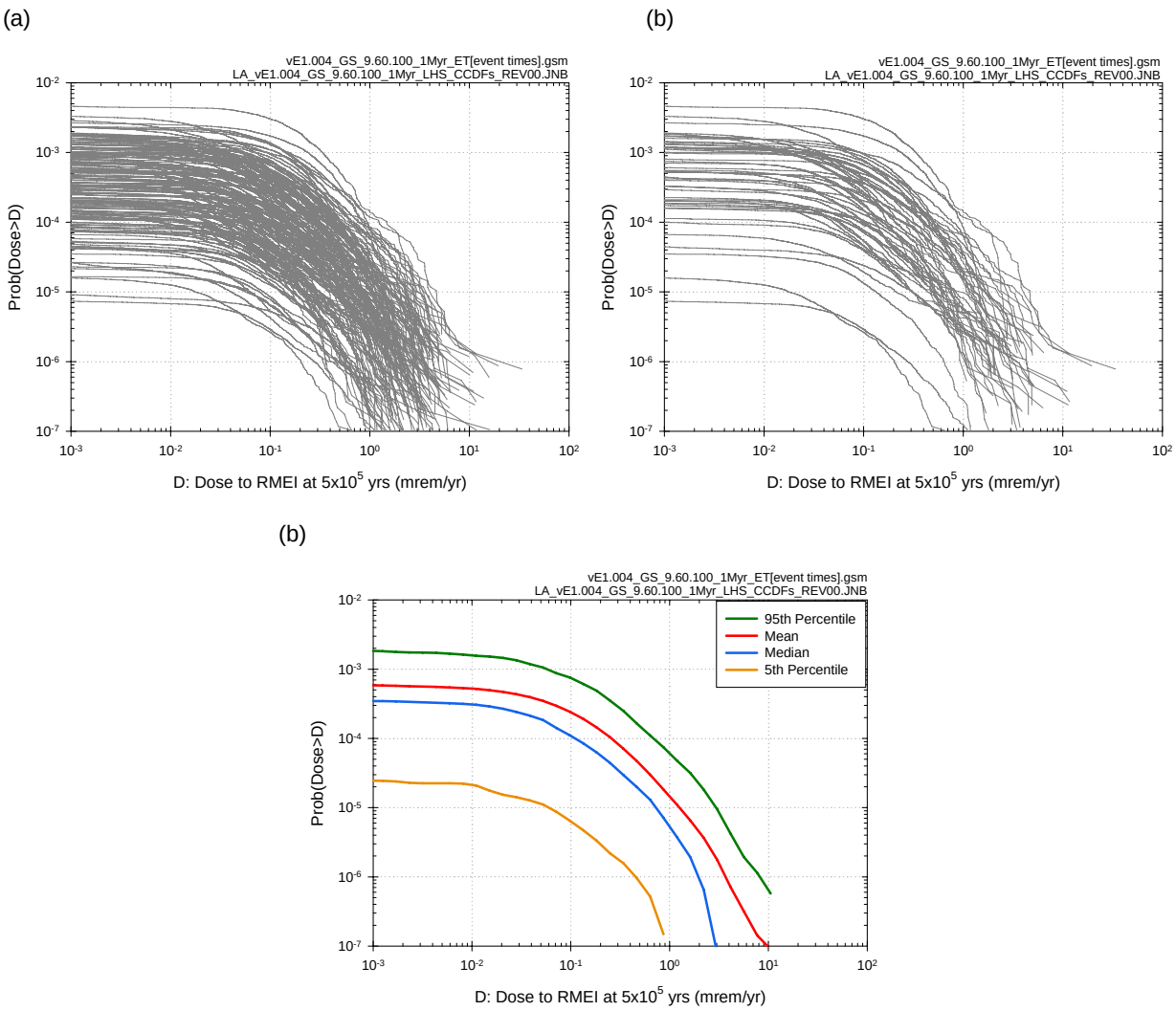

Source: Ouput DTNs: MO0709TSPAPLOT.000 [DIRS 183010]; and MO0709TSPAREGS.000 [DIRS 182976].

Figure J7.3-17. Results associated with D_{IE}(500,000 yr|$\mathbf{a}_{IE}$, $\mathbf{e}_M$) obtained with sampling-based (Monte Carlo) procedures for an LHS of size $nLHS$ = 300: (a) CCDFs for D_{IE}(10^4 yr|$\mathbf{a}_{IE}$, $\mathbf{e}_{Mi}$) with exceedance probabilities $p_A[D < D_{IE}(500{,}000 \text{ yr}|\mathbf{a}, \mathbf{e}_{Mi})|\mathbf{e}_{Ai}]$ defined in Equation J7.3-20 for i = 1, 2, …, $nLHS$ = 300, (b) CCDFs for D_{IE}(500,000 yr|$\mathbf{a}_{IE}$, $\mathbf{e}_{Mi}$) with exceedance probabilities $p_A[D < D_{IE}(500{,}000 \text{ yr}|\mathbf{a}, \mathbf{e}_{Mi})|\mathbf{e}_{Ai}]$ defined in Equation J7.3-20 for i = 1, 2, …, 50, and (c) expected (mean) CCDF and quantile curves, q = 0.05, 0.5, 0.95, for CCDFs in (a).

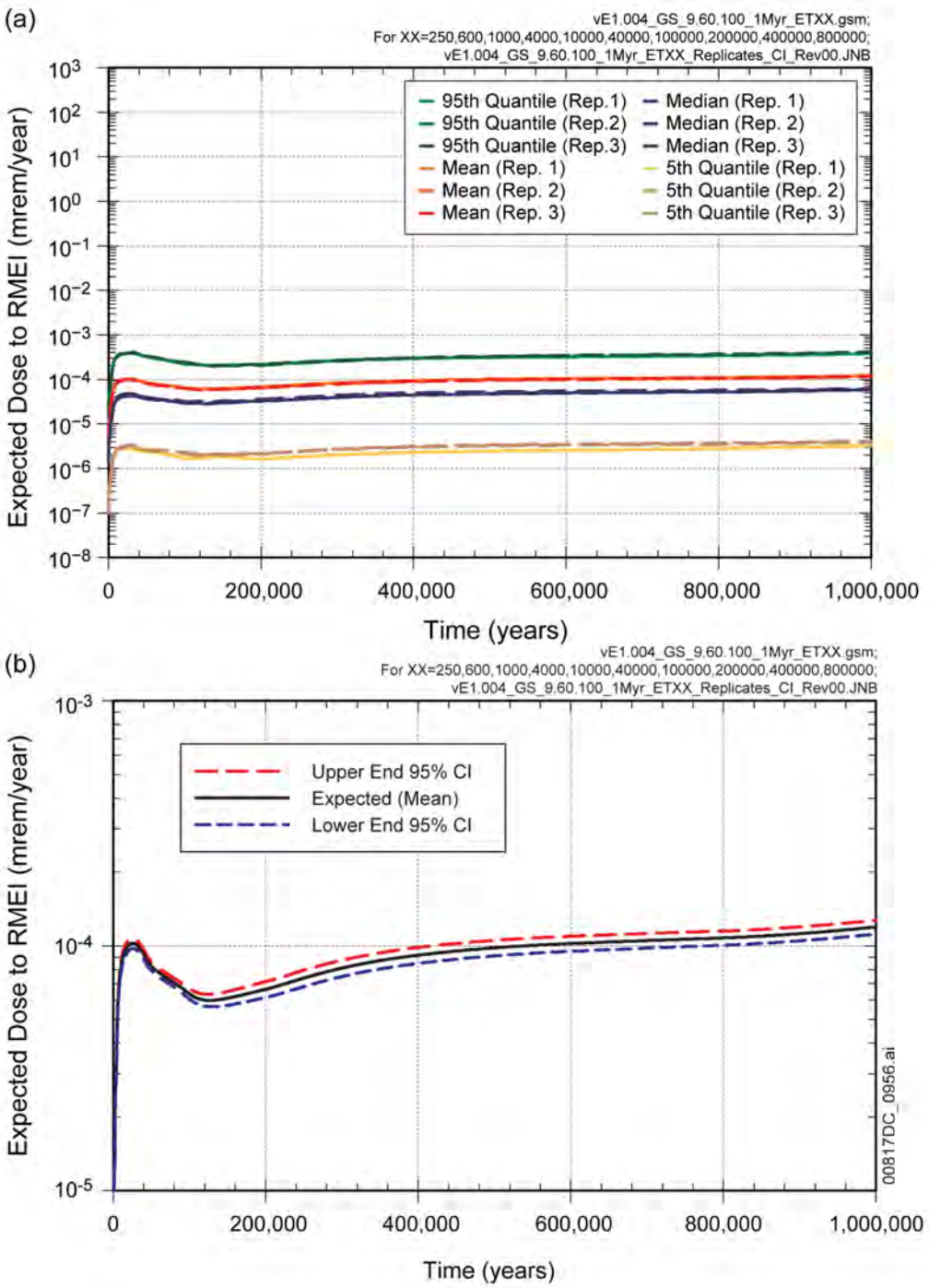

Source: Ouput DTNs: MO0709TSPAPLOT.000 [DIRS 183010]; and MO0709TSPAREGS.000 [DIRS 182976].

Figure J7.3-18. Assessment with replicated sampling of numerical error associated with use of an LHS of size *nLHS* = 300 to determine epistemic uncertainty in expected dose $\bar{\bar{D}}_{IE}(\tau)$ to RMEI for $0 \le \tau \le 10^6$ yr that results when only igneous eruptive events are considered: (a) Replicated estimates of expected (mean) dose $\bar{\bar{D}}_{IE}(\tau)$ and quantiles $Q_q[\bar{D}_{IE}(\tau|\mathbf{e})]$, q = 0.05, 0.5, 0.95, and (b) confidence intervals for estimates of expected (mean) dose $\bar{\bar{D}}_{IE}(\tau)$.

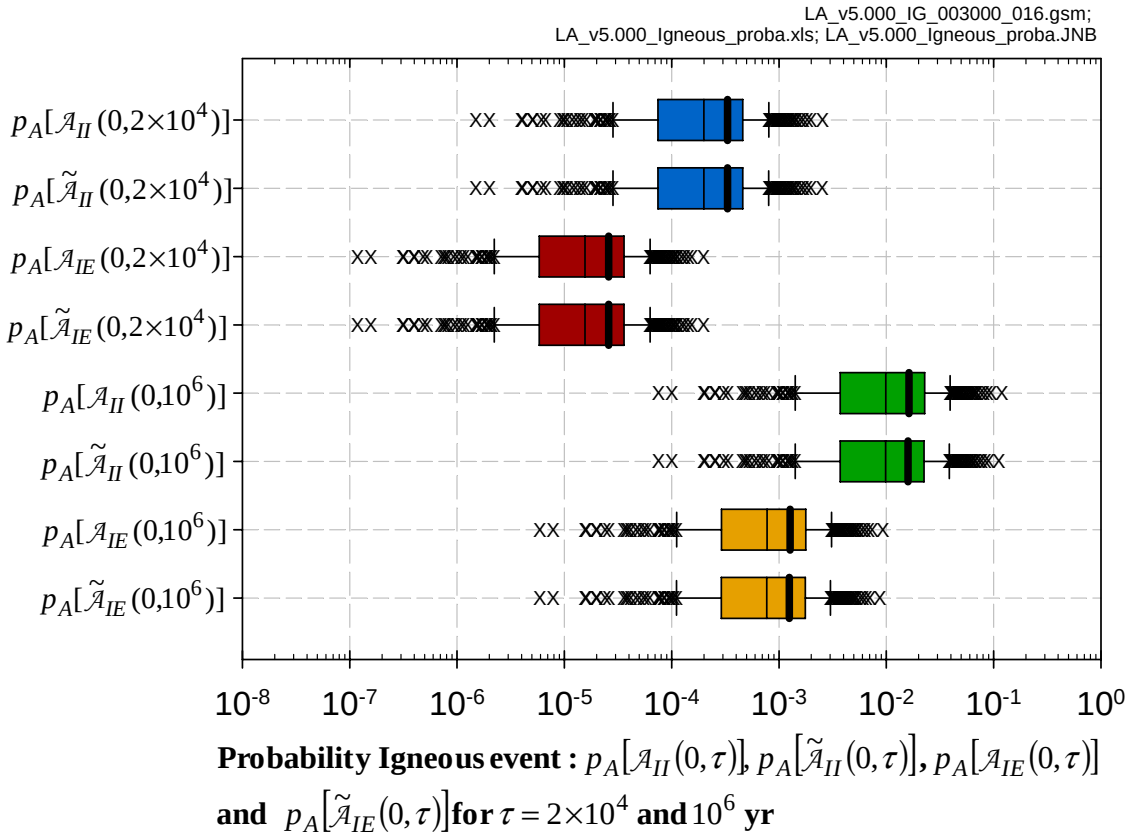

Source: Ouput DTNs: MO0709TSPAPLOT.000 [DIRS 183010]; and MO0709TSPAREGS.000 [DIRS 182976].

Figure J7.5-1. Box plots summarizing probabilities $p_A[\mathcal{A}_{II}(0, \tau)|\mathbf{e}_{Ai}]$, $p_A[\tilde{\mathcal{A}}_{II}(0, \tau)|\mathbf{e}_{Ai}]$, $p_A[\mathcal{A}_{IE}(0, \tau)|\mathbf{e}_{Ai}]$ and $p_A[\tilde{\mathcal{A}}_{IE}(0, \tau)|\mathbf{e}_{Ai}]$ for scenario classes $\mathcal{A}_{II}(0, \tau)$, $\tilde{\mathcal{A}}_{II}(0, \tau)$, $\mathcal{A}_{IE}(0, \tau)$ and $\tilde{\mathcal{A}}_{IE}(0, \tau)$ defined for the time intervals [0, 20,000 yr] and [0, 1,000,000 yr] obtained with LHS of size *nLHS* = 300.

INTENTIONALLY LEFT BLANK